Summer 2018

Local Adaptation Signatures in Thermal Performance of the Temperate Coral Astrangia poculata

Hannah Elise Aichelman
Old Dominion University, hannahaichelman@gmail.com

LOCAL ADAPTATION SIGNATURES IN THERMAL PERFORMANCE OF THE TEMPERATE CORAL *ASTRANGIA POCULATA*

by

Hannah Elise Aichelman
B.S. May 2014, University of North Carolina at Chapel Hill

A Thesis Submitted to the Faculty of
Old Dominion University in Partial Fulfillment of the
Requirements for the Degree of

MASTER OF SCIENCE

BIOLOGY

OLD DOMINION UNIVERSITY
August 2018

Approved by:

Daniel J. Barshis (Director)

David Gauthier (Member)

Richard Zimmerman (Member)

ABSTRACT

LOCAL ADAPTATION SIGNATURES IN THERMAL PERFORMANCE OF THE TEMPERATE CORAL *ASTRANGIA POCULATA*

Hannah Elise Aichelman
Old Dominion University, 2018
Director: Dr. Daniel J. Barshis

The Northern Star Coral (*Astrangia poculata*) is an understudied temperate scleractinian coral that provides unique opportunities to understand the roles of phenotypic plasticity and local adaptation in coral physiological tolerance limits. *Astrangia poculata* inhabits hard bottom ecosystems from the northwestern Atlantic to the Gulf of Mexico and withstands an annual temperature range up to 20°C. Additionally, *A. poculata* is facultatively symbiotic and co-occurs in both symbiotic ("brown") and aposymbiotic ("white") states. Here, brown and white *A. poculata* were collected from Virginia (VA) and Rhode Island (RI), USA and exposed to heat (18-32°C) and cold (18-6°C) temperature assays during which photosynthesis (P), respiration (R), and symbiont photochemical efficiency (F_v/F_m) were measured. Thermal performance curves (TPCs) of respiration revealed differences consistent with local adaptation of the RI and VA populations to their natal thermal environments. RI corals exhibited higher respiration rates overall, and higher respiration at 6, 15, 18, 22, and 26°C. Additionally, thermal optimum (T_{opt}) analyses show a 3.76°C (brown) and 6.88°C (white) greater T_{opt} in the VA population, corresponding to the warmer *in situ* thermal environment in VA. In contrast to respiration, no origin effect was detected in photosynthesis rates or F_v/F_m, suggesting a possible host-only signature of local adaptation. This study is the first to consider *A. poculata*'s response to both heat and cold stress across symbiotic states and geography and provides insight into the effects of future climate change on valuable hard bottom communities along the East Coast of the US.

This thesis is dedicated to my Dad, for inspiring my sense of adventure and providing continual support throughout the roller coaster of graduate school. I love you to the moon and back.

ACKNOWLEDGMENTS

In the last month of writing and defending this thesis, I have been overwhelmed by the amount of love and encouragement from my community and reminded that this work would not have been possible without the incredible support of many people. First and foremost, thank you to my advisor Dan for helping me to grow as a scientist and as a human over the last two years. This degree has been an incredible adventure, and it is an honor to be your first Master's student. I look forward to collaborating and nerding out on many future projects. I also extend heartfelt thanks to the other members of my committee, Dick Zimmerman and Dave Gauthier. Dick, thank you for reminding me to take a step back in order to truly understand my science, and for holding me to a higher standard. Dave, thank you for being a sounding board for all things molecular and most importantly, for teaching me how to brew delicious beer.

There are also many folks not on my committee that contributed enormously to the successful completion of this project. Thank you to Sean Grace at Southern Connecticut State University for his gracious Rhode Island field support, especially for introducing me to diving in Narragansett Bay and for sharing temperature data. I would also like to extend appreciation to Koty Sharp, Randi Rotjan, Sean Grace and the annual *Astrangia* Workshop hosted by Roger Williams University for fostering creative conversations and collaborations leading to this work. The experiments presented here would not have been possible without help from many ODU undergraduates and volunteers, including Kristina Bounds, James Murphy, Tyler Harman, Robbie Rowe, Sandrine Boissel, and Ingrid Fuquene. Additionally, I received advice and R guidance from Dr. Hollie Putnam at the University of Rhode Island and Dr. Dan Padfield at the

University of Exeter regarding the statistical analyses of the thermal performance curve data presented here – thank you.

To my incredible friends and family. First, thank you Dad, Julie, and Jay for being the best family around. Even though I will always miss being in the same city as you all, thank you for supporting me as I pursue a career in science. Thank you to my lab mate, friend, adventure partner, and all around amazing person Courtney, without whose enthusiasm and love I certainly would have gone crazy throughout this process. Also, endless thanks to my tribe of badass ODU grad student friends. Jeri, Jamie, and Emily, there are no words for how thankful I am to have found you. Thank you for always being willing to drink rosé, go on a brewery tour, or escape to the wilderness. I can't wait to see the incredible things you all accomplish in your careers.

Last but certainly not least; this thesis would not have been possible without financial support from the Virginia Sea Grant Graduate Research Fellowship (VASG), which fully funded my Master's degree. Thank you to everyone at VASG, especially Sam Lake and Troy Hartley, for the amazing opportunity to be a Virginia Sea Grant fellow. Additionally, I received support from small grants from the PADI Foundation, the Hollis Gear Award, and the ODU Biology Graduate Student Organization.

NOMENCLATURE

P	Photosynthesis
R	Respiration
TPC	Thermal Performance Curve
T_{opt}	Thermal optimum
F_v/F_m	Symbiont photochemical efficiency
P_{gross}	Gross Photosynthesis (units of μmol $O_2 cm^2 h^{-1}$)
P_{net}	Net photosynthesis (units of μmol $O_2 cm^2 h^{-1}$)
R_{corr}	Dark respiration corrected for rates of commensals (units of μmol $O_2 cm^2 h^{-1}$)
P_{corr}	Gross photosynthesis corrected for rates of commensals (units of μmol $O_2 cm^2 h^{-1}$)
P_{max}	Maximum rate of photosynthesis (units of μmol $O_2 cm^2 h^{-1)}$
RI	Rhode Island
VA	Virginia
SST	Sea surface temperature (units of °C)
OTU	Operational Taxonomic Unit

TABLE OF CONTENTS

PAGE

LIST OF TABLES

LIST OF FIGURES

Figure Page

INTRODUCTION

Local adaptation is the specialization of populations to local environmental conditions through natural selection and represents equilibrium between divergent selection pressures and the homogenizing effects of gene flow (e.g., Kawecki and Ebert, 2004; Sanford and Kelly, 2011). Historically, local adaptation in the marine environment was believed to be rare due to the misconception that marine populations were well-mixed as a result of high gene flow (Sanford and Kelly, 2011). However, several recent studies on marine invertebrates have demonstrated population differentiation consistent with local adaptation at a variety of spatial scales. For example, adaptation to local thermal environments was observed in corals in both American Samoa (Barshis et al., 2010; Bay and Palumbi, 2014; Palumbi et al., 2014) and the Florida Keys (Kenkel et al., 2013), as well as in European green crabs in the native and invasive range (Tepolt and Somero, 2014). Temperature is an environmental parameter of particular interest to biologists, as it plays a major role in shaping an organism's growth, survival, reproduction, and population density; as well as species distributions and patterns of species diversity (Angilletta, 2009; Hochachka and Somero, 2002; Schulte et al., 2011). Local adaptation to distinct thermal environments along a species' range could therefore result in differential responses or susceptibility to temperature variation throughout that range. These population-level responses to environmental variability and thermal conditions are of particular concern to researchers, and understanding the mechanisms of how temperature affects populations and their distribution will assist in predicting the "winners" and "losers" under future climate change conditions (Somero, 2010).

Thermal performance curves (TPCs) are often used to quantify the effect of temperature on an organism's performance within its zone of tolerance (Angilletta, 2009; Huey and Stevenson, 1979; Schulte et al., 2011). TPCs tend to exhibit the same general shape, in which performance increases with temperature until some thermal optimum (T_{opt}) and then rapidly decreases (Angilletta Jr et al., 2002; Angilletta, 2009; Huey and Kingsolver, 1989; Huey and Kingsolver, 1993; Huey and Stevenson, 1979). TPCs have been used previously to understand the response of different populations to increasing temperatures (e.g., Gardiner et al., 2010) and to predict organism responses to climate change (Schulte et al., 2011). When comparing TPCs

from multiple populations of the same species across a thermal gradient, several patterns could be expected (Angilletta, 2009; Gardiner et al., 2010). First, thermal optima could be adapted to the local thermal environment, meaning that populations from warmer sites will outperform populations from cooler sites at warmer temperatures, and vice versa (Angilletta, 2009). Second, populations from warmer sites could outperform populations from colder sites at all temperatures (cogradient variation, Conover et al., 2009). Third, populations from cold sites could outperform populations from warm sites at all temperatures (countergradient variation, Angilletta, 2009). Finally, there could be no difference in performance between populations (Angilletta, 2009; Gardiner et al., 2010). It is imperative to understand how temperature affects different populations when predicting how a species may respond to future environmental change at large spatial scales (Gardiner et al., 2010; Schulte et al., 2011).

The northern star coral *Astrangia poculata* (= *A. danae*; Peters et al., 1988) is a temperate scleractinian coral that has two primary characteristics which distinguish it from tropical corals and make it an interesting species for studying thermal susceptibilities. First, *A. poculata* is facultatively symbiotic and exists both in symbiosis with the endosymbiotic algae *Symbiodinium psygmophilum* (symbiotic or brown; LaJeunesse et al., 2012) and without (aposymbiotic or white). This facultative symbiosis enables independent characterizations of the relative role that coral hosts and symbionts play in thermal tolerance, as the response of the host can be isolated in experiments using aposymbiotic colonies. Second, *A. poculata* has an extensive range, inhabiting hard bottom environments from the Gulf of Mexico to Cape Cod, Massachusetts (Peters et al., 1988; Thornhill et al., 2008). Therefore, *A. poculata* populations span a wide range of environmental conditions, particularly temperature, both within and among sites. For example, in Rhode Island (RI), *A. poculata* thrives in temperatures that reach 27°C in the summer and drop as low as 0°C in the winter (Dimond and Carrington, 2007). This characteristic is drastically different from tropical corals, which are limited to living within a narrow thermal range of less than 10°C (Veron, 2000). The majority of previous studies on *A. poculata* have focused on sites from the northern end of this species' range, including RI (e.g., Burmester et al., 2017; DeFilippo et al., 2016; Dimond and Carrington, 2007; Jacques, 1983; Jacques, 1980) and Massachusetts (e.g., Holcomb et al., 2012; Holcomb et al., 2010; Ries, 2011). Although some Mid-Atlantic shipwrecks are extensively covered by *A. poculata* (up to 75%, personal observation), there is very little known about this species in the more central and southern parts of its range.

Here, I conducted a common garden experiment to look for phenotypic evidence of local adaptation in thermal performance of the temperate coral *A. poculata.* The goal was to investigate whether thermal performance of *A. poculata* varies across a latitudinal thermal gradient or by symbiotic status by measuring metabolic rates (respiration, R and photosynthesis, P) of brown and white *A. poculata* as well as the quantum yield of photochemistry in photosystem II (PSII), hereafter referred to as photochemical efficiency (F_v/F_m, reviewed by Fitt et al., 2001), at a range of temperatures (6-32°C) from two sites along the species' range (Virginia, VA and Rhode Island, RI; Fig. 1). Because sea surface temperatures (SST) in VA are consistently warmer over the course of the year (Fig. 2A), I hypothesized that VA corals would be adapted to warmer temperatures, and therefore out-perform RI corals at warmer temperatures and exhibit a higher thermal optimum (T_{opt}; the first scenario outlined above). This work assesses the potential for local adaptation of coral physiology to environmental conditions at a regional spatial scale and has implications for understanding how *A. poculata* on the east coast of the United States could respond to future temperature increases associated with climate change. The vulnerability of temperate corals to climate change, particularly *A. poculata*, is greatly under-studied, even though recent warming was greater in the North Atlantic as compared to other ocean basins (Rhein et al., 2013).

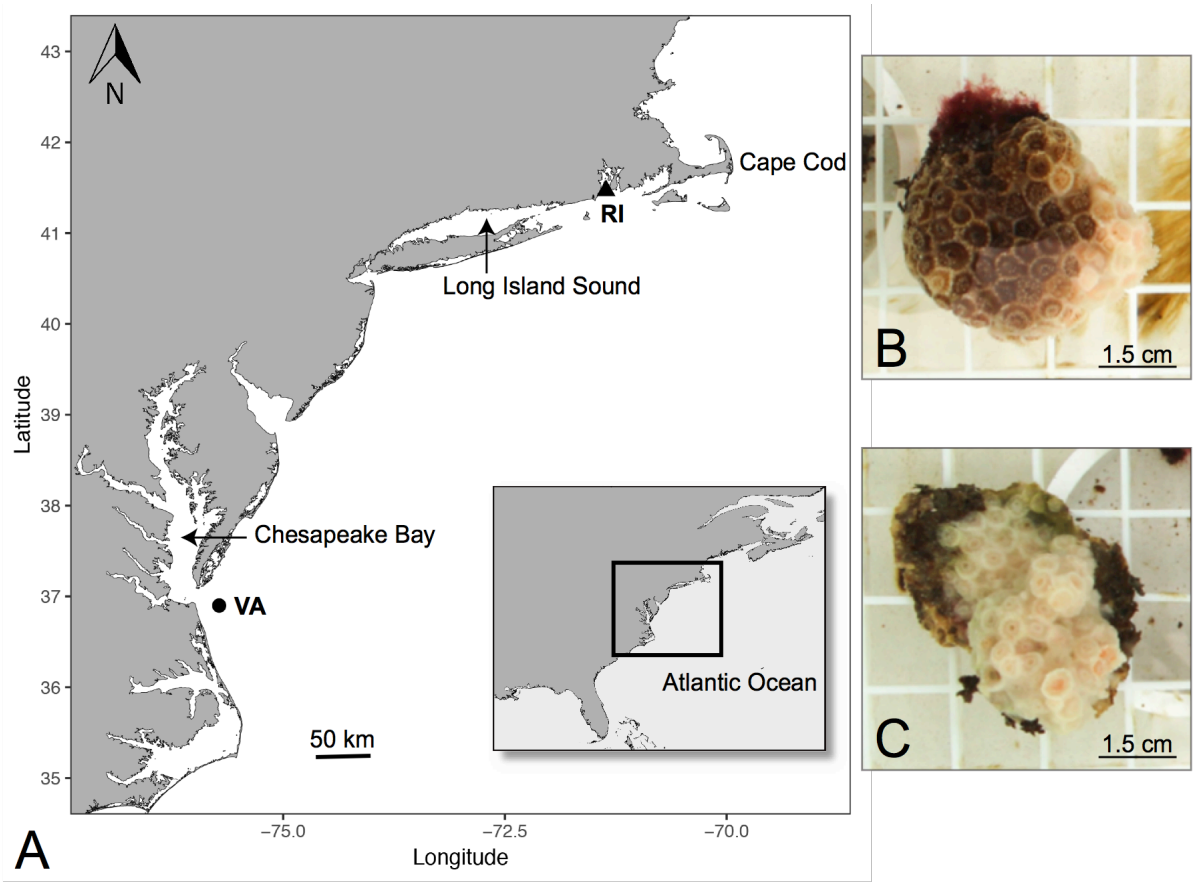

Fig. 1. Map of sampling sites and study species. (A) Map showing location of *Astrangia poculata* collections (Virginia = VA, Rhode Island = RI). **(B)** Example of symbiotic ("brown") colony of *Astrangia poculata.* (C) Example of aposymbiotic ("white") colony of *Astrangia poculata.*

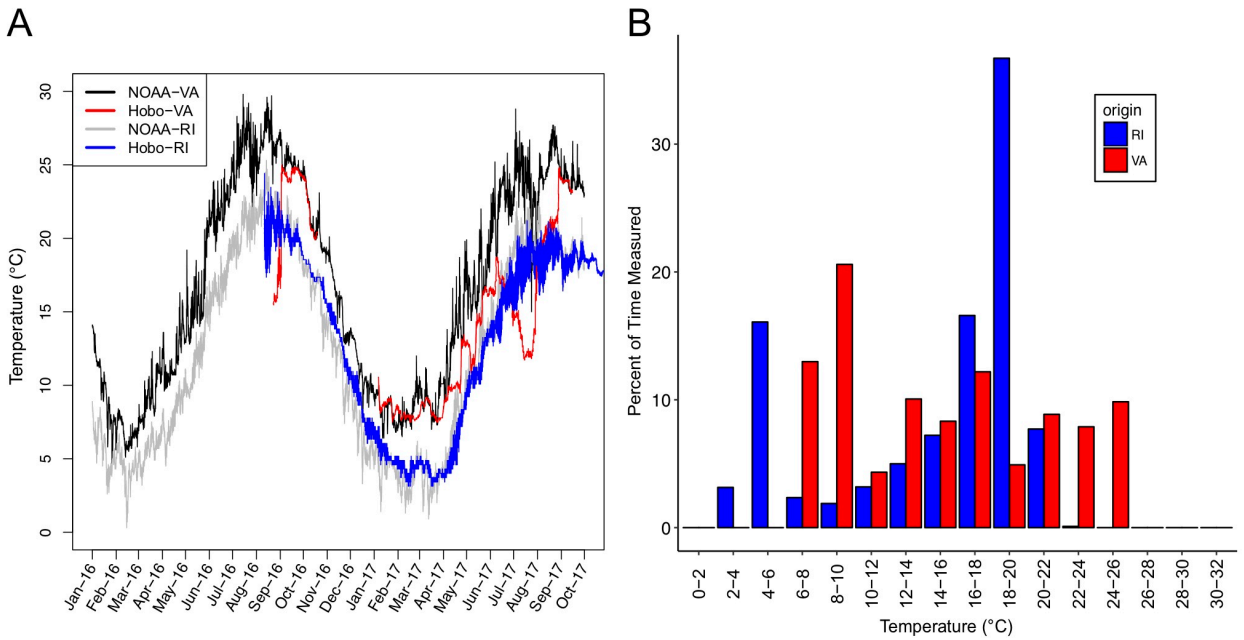

Fig. 2. Comparison of VA and RI thermal environment. (A) Sea surface temperature (SST) and temperature at collection depth of VA and RI sites between January 2016 and October 2017. SST of VA and RI sites was extracted from the Cape Henry, VA and Newport, RI NOAA data buoys (black and gray lines, respectively). Temperature at the collection depths of the VA and RI sites (red and blue lines, respectively) was recorded by Hobo Pendant temperature loggers (*Onset Computer Corp*.). **(B)** Percent of time that each site (VA and RI) spent at 2°C intervals between 0 and 32°C. The data included is the same Hobo logger data as that represented by the blue and red lines in panel (A).

METHODS

CORAL COLLECTION AND TRANSPORTATION

In May and June 2017, 10 brown and 10 white *Astrangia poculata* colonies were collected from Virginia (VA) and Rhode Island (RI), USA (Fig. 1). VA colonies were collected from the wreck of the J.B. Eskridge (36°53’57.1”N 75°43’20.6”W) on May 26 and June 2, 2017 at 20 m depth. All VA colonies were transported to the Old Dominion University (ODU) Aquatics Facility and placed in a common garden aquarium within 6 hours of collection. RI colonies were collected from Fort Wetherill State Park (41°28’38.7”N 71°21’36.3”W) on June 9, 2017 from a depth of approximately 11 m. RI colonies were maintained overnight at the Roger Williams University Aquatics Facility in a recirculating seawater aquarium (temperature = 18°C, salinity = 35 ppt) and then transported by car in an aerated aquarium to ODU the next day. All VA and RI colonies were collected using a hammer and chisel and were separated by at least 0.5 m to ensure the collection of distinct individuals. VA corals were collected under Virginia Marine Resources Commission permit #17-017, while no permit was required for collection of RI corals.

IN SITU TEMPERATURE ENVIRONMENT

VA *in situ* temperature was recorded every 15 minutes between August 23, 2016 and October 19, 2016 and again between January 6, 2017 and September 14, 2017 by Hobo Pendant® Temperature Data Loggers (Onset Computer Corporation, Bourne, MA, USA) deployed on the wreck of the J.B. Eskridge (Fig. 2A). RI *in situ* temperature was recorded every 15 or 16 minutes by StowAway TidbiT Temperature Data Loggers (Onset Computer Corporation, Bourne, MA, USA) between August 11, 2016 and November 7, 2017 deployed at the collection site (RI data courtesy of Dr. Sean Grace, Southern Connecticut State University). *In situ* temperature was compared to sea surface temperature (SST) recorded by the NOAA data buoys closest to the collection sites (NOAA National Data Buoy Center; Fig. 2A). VA SST data were extracted from the Cape Henry buoy (station 44099, 36°54'55"N 75°43'12"W), and RI SST data were extracted from the Newport, Rhode Island buoy (station 8452660, 41°30'16"N 71°19'34"W).

CORAL RECOVERY AND ACCLIMATION

Upon arrival at the ODU Aquatics Facility, all VA and RI individuals were placed in a common garden aquarium and maintained at 15°C (approximate temperature at time of collection for both sites) and salinity of 35 ppt. Whole colonies were allowed to acclimate at ambient conditions (15°C and 35 ppt) for at least 10 days before fragmenting. Corals were fragmented over three days (June 19 - 21, 2017) using a high-speed cut off tool (Chicago Pneumatic, Rock Hill, SC, USA) fitted with a diamond tip circular blade, then affixed to circular Plexiglas stands using InstaCure ethyl cyanoacrylate gel (IC-Gel; Bob Smith Industries Inc., Atascadero, CA, USA). As many non-coral organisms as possible (i.e., algae, sponge, and other coral-associated organisms) were removed from the coral pieces during the fragmentation process using the same high-speed cut off tool and diamond tip circular blade.

After fragmenting, all corals were allowed to recover at 15°C for at least one week, after which temperature was increased 1°C day^{-1} until the target 18°C was achieved. Coral fragments were then acclimated to the new ambient conditions for another week before respirometry experiments began (16 days recovery/acclimation post fragmentation, at least 24 days total recovery/acclimation). The ambient temperature of 18°C was chosen for these experiments as it is a moderate temperature within the natural thermal range of both populations (Fig. 2) and has been previously reported in the literature as a control temperature for RI *A. poculata* (e.g., Burmester et al., 2017).

EXPERIMENTAL DESIGN

A series of 16 distinct ramp experiments were performed to determine the thermal performance curves (TPCs) of photosynthesis (P), respiration (R) and symbiont photochemical efficiency (F_v/F_m) of VA and RI populations of *A. poculata*. The sixteen experiments consisted of four categories of ramp experiments: 1) a heat ramp of the coral holobiont (18 to 32°C), 2) a cold ramp of the coral holobiont (18 to 6°C), 3) a heat ramp of the coral skeleton only (18 to 32°C), and 4) a cold ramp of the coral skeleton only (18 to 6°C). Following Jacques (1983), coral tissue was airbrushed off the skeleton and used in the heat and cold skeleton ramps to obtain metabolic rates of the community of commensal organisms housed in the skeleton independent of the host and *Symbiodinium.* These skeleton only metabolic rates were subtracted from the holobiont metabolic rates to obtain a corrected measure (R_{corr} and P_{corr}) of the coral host and

symbiont metabolism. Each ramp experiment included 8 unique *A. poculata* individuals (i.e., genets), including 2 VA-brown, 2 VA-white, 2 RI-brown, and 2 RI-white fragments. When possible, the *A. poculata* individuals used in these experiments were cut into 4 fragments, allowing all genets to be represented in all four ramp categories. This was the case for all VA individuals; however, because RI *A. poculata* individuals were generally smaller than VA, it was difficult to cut every RI coral into four fragments of sufficient size. Therefore, a total of 10 RI-brown individuals and 9 RI-white individuals were used in these experiments. The four categories of ramp experiments were each repeated four times, for a total of 16 thermal performance ramps, all of which took place within 20 days of each other in July 2017.

Each of the 16 ramp experiments proceeded as follows. At approximately 07:30, eight experimental coral fragments were moved from the common garden aquarium to the experimental aquarium and randomly assigned to one of 9 respirometry chambers. Before transferring, temperature and salinity of both the common garden and experimental aquaria were measured to ensure these parameters were equivalent (18 ± 0.2°C and 35 ppt). Following at least a 30-minute dark acclimation, oxygen consumption in the dark was recorded for 20 minutes to estimate dark respiration (R). Next, each chamber was flushed with non-chamber water and F_v/F_m was measured in triplicate for each fragment. Following the F_v/F_m measurements, chambers were re-sealed and oxygen evolution in the light (400 μmol photons $m^{-2}s^{-1}$, supplied by a single 165 W LED aquarium light; GalaxyHydro, Roleadro, Shenzhen, China) was recorded for 20 minutes to estimate net photosynthesis (P_{net}), after which the temperature was either increased or decreased to the next target temperature (heat or cold ramp, respectively). The specifics of collection and analysis of the R, F_v/F_m, and P_{net} measurements are detailed below.

The irradiance used here was chosen based on both a photosynthesis-irradiance (P vs. E) experiment, as well as previous photosynthesis experiments on RI *A. poculata* (Jacques, 1983). Here, P_{gross} was measured at 8 light intensities between 5 and 845 μmol photons $m^{-2}s^{-1}$ in four brown VA individuals. Using the CFTOOL in MATLAB (vR2016b), the least squares best fit was calculated for irradiance and P_{gross} for the exponential equation (Fig. S1). The light level of 400 μmol photons $m^{-2}s^{-1}$ was chosen for the ramp experiments because this irradiance elicited the maximum photosynthesis rate (P_{max}), was well below light levels that induced photoinhibition (Fig. S1), and agreed with the findings of Jacques (1983).

This sequence of dark acclimation, R, F_v/F_m, P_{net}, and temperature change was repeated at five temperatures for both the heat (18, 22, 26, 29, 32°C) and cold (18, 15, 12, 9, 6°C) ramp experiments. A custom-programmed Arduino® (Arduino AG, Somerville, MA, USA) was used to control the water temperature during the ramp experiments (code assembled by D. Barshis). During P, R, and F_v/F_m measurements, water temperature was controlled within ±0.5°C of the set temperature. Water temperature was monitored throughout each ramp experiment with a Hobo Pendant® Temperature Data Logger (Onset Computer Corporation, Bourne, MA, USA; Fig. S2).

Once all measurements were completed at the final temperature of each ramp experiment, the fragments were photographed, immediately frozen in liquid nitrogen, wrapped in aluminum foil and placed in an -80°C freezer for long-term storage.

TRAIT MEASUREMENTS

RESPIROMETRY

Metabolic rates (R and P_{net}) were determined by measuring changes in dissolved oxygen (O_2) concentration using a fiber-optic O_2 sensor connected to a 10-channel Fiber Optic Oxygen Transmitter (OXY-10 mini, Pre-Sens Precision Sensing GmbH, Regensburg, Germany) in a custom-made UV-transparent acrylic 9-chamber respirometry system. The OXY-10 mini instrument was calibrated in accordance with the supplier's manual (Oxy-10 mini with Oxygen-Sensitive Spot PSt3, Pre-Sens Precision Sensing GmbH, Regensburg, Germany). Each of the nine chambers was mounted in a Plexiglas base, submerged in a recirculating water bath in the experimental aquarium, positioned on a magnetic stir plate, and a magnetic stir bar was used to maintain constant and turbulent water flow throughout the measurements. Oxygen evolution was recorded in a blank chamber (no coral fragment) during each measurement, and this blank metabolic rate was subtracted from the rate calculated in the experimental chambers at the corresponding temperature and measurement to correct for any metabolic activity of microbes in the water or instrument drift.

Raw oxygen evolution was recorded by associated Pre-Sens software (version Oxy10v3_33fb) and corrected for temperature and salinity of the water using a custom python script (written by D. Barshis and H. Aichelman and based on the correction spreadsheet provided by Pre-Sens). Metabolic rates were calculated from these corrected raw O_2 values using the

LoLinR package (Olito et al., 2017) in R v3.4.0 (R Core Team, 2017). This package utilizes local linear regression techniques to estimate metabolic rates from time series data in a robust and reproducible way (Olito et al., 2017). Following correction of the O_2 evolution values and calculation of the raw metabolic rate, the metabolic rate for each fragment was normalized to surface area of the corresponding coral fragment (see below) and corrected for drift, therefore all metabolic rates presented here are in units of μmol O_2 cm^2 h^{-1}. Gross photosynthesis (P_{gross}), the amount of oxygen produced in the light after accounting for respiratory demands, was calculated by subtracting dark respiration from P_{net}.

HOLOBIONT

The day before each ramp experiment, several physiological traits were recorded for each experimental fragment. All fragments were cleaned to remove any algal growth and then buoyant weighed in triplicate as described by Davies (1989). Additionally, wet weight of each coral fragment was measured with a NIST-calibrated scale and recorded. Lastly, each fragment was photographed the day before and immediately upon completion of each ramp experiment. These photos were used to quantify surface area of each experimental fragment, which was estimated using the image analysis software ImageJ (Schindelin et al., 2015). This 2-D analysis was found to produce a reasonable measure of *A. poculata* surface area, as the majority of colonies collected for this experiment were encrusting, and during fragmentation corals were cut into pieces as uniform in height as possible. These surface area measurements were also used to correct metabolic rates, as described above.

SYMBIODINIUM

In order to quantify *Symbiodinium* performance throughout the ramp experiments, photochemical efficiency (F_v/F_m) was measured in triplicate for each experimental fragment at each temperature of all ramp experiments using a pulse-amplitude modulated fluorometer (JUNIOR-PAM; Heinz Walz GmbH, Effeltrich, Germany) following at least 40 min of dark adaptation. Dark-adapted F_v/F_m can be used as an indicator of *Symbiodinium* stress, and should decrease during thermal stress (Falkowski and Raven, 2007; Fitt et al., 2001; Thornhill et al., 2008; Warner et al., 1996).

The same photos described above were also used to approximate chlorophyll and symbiont densities of each fragment following the protocol presented by Winters et al. (2009). Briefly, using the MATLAB macro 'AnalyzeIntensity', mean red channel intensity was

calculated for 20 quadrates of 25 x 25 pixels for each fragment and used as a measure of brightness (i.e., higher brightness indicates fewer algal pigments).

AQUARIA CONDITIONS

Before each ramp experiment, all experimental corals were maintained in a 325-gallon common garden aquarium with artificial seawater mixed to 35 ppt using Crystal Sea® Bioassay salt (Marine Enterprises International, Baltimore, MD, USA) and deionized (DI) water. Temperature was maintained at the target temperature ±0.5°C using an AquaLogic® temperature controller (AquaLogic, San Diego, CA, USA) in combination with an in-line water chiller (Delta Star®, AquaLogic, San Diego, CA, USA) and 1500 W SmartOne® Max Bottom immersion heater (Process Technology, Willoughby, Ohio, USA). The common garden aquarium was equipped with a filter sock for mechanical filtration, protein skimmer for removal of organic material, and powerheads (Tunze® Turbelle, Penzburg, Germany) to maintain flow.

The respirometry experiments were run in a separate experimental aquarium equipped with the custom metabolic chamber set-up previously described. As in the common garden aquarium, artificial seawater was mixed to 35 ppt using Crystal Sea® Bioassay salt. Temperature was manipulated using a custom-programmed Arduino® (code assembled by D. Barshis) connected to the same style heater and chiller as the common garden aquarium.

Routine maintenance of *A. poculata* before the ramp experiments included feeding 3x week^{-1} with freshly hatched brine shrimp (*Artemia sp.*), which were distributed over the surface of each fragment using a Pasteur pipette. However, before respirometry experiments, corals were starved for 24 hours to standardize metabolic response during ramps. Additionally, weekly water changes of 15% in the common garden aquarium and 100% in the experimental aquarium were performed. Temperature and salinity were monitored daily in both aquaria using a NIST-calibrated thermometer and a refractometer, respectively. Additional nutrient parameters, including nitrate, nitrite, ammonium, phosphate, calcium, and magnesium, were monitored bi-weekly using API test kits (Mars Fishcare North America Inc., Chalfont, PA, USA).

SYMBIONT GENOTYPING

In order to identify the *Symbiodinium* species associated with *A. poculata* from VA and RI, genomic DNA was isolated from n=10 VA and n=10 RI brown individuals following a CTAB-chloroform extraction protocol (Baker and Cunning, 2016) and quantified using a Nanodrop 2000 Spectrophotometer (Thermo Scientific, Waltham, MA, USA). The internal transcribed spacer region 2 (ITS2) was amplified using custom primers incorporating *Symbiodinium* specific ITS-2-dino-forward and its2rev2-reverse regions (as in Baumann et al., 2017) and the following PCR profile: 95°C for 5 min, followed by 35 cycles of 95°C for 40s, 59°C for 2 min, 72°C for 30s, and a final extension of 7 min at 72°C. Each 20 µL reaction contained 2 µL DNA template, 7.8 µL Milli-Q H_2O, 10 µL of 2X BioMix^{TM} Red (Bioline USA, Taunton, MA, USA), 1 µM forward and 1 µM reverse primers. The PCR products were cleaned using the ExoSAP-IT PCR Product Cleanup Kit according to manufacturer's instructions (Affymetrix Inc., Santa Clara, CA, USA) before a second set of PCRs, which incorporated sequence primers and unique barcodes to each sample using Illumina's Nextera XT Adapter Kit (Illumina, San Diego, CA, USA) *sensu* Kenkel et al. (2013). Samples were pooled and sequenced using a 250bp paired-end MiSeq Nano Reagent Kit version 2 (Illumina, San Diego, CA, USA) on ODU's Illumina MiSeq.

Raw reads were de-multiplexed, and counts of distinct Operational Taxonomic Units (OTUs) as well as sequence variants were identified using the DADA2 pipeline (Callahan et al., 2016) in R v3.4.0 (R Core Team, 2017). Four unique OTUs represented across five individuals (3 VA-brown and 2 RI-brown) passed the filtering steps of DADA2. The representative *Symbiodinium* species of each of the four OTUs was determined by a BLASTn search against the GenBank (NCBI) nucleotide reference collection. The individuals used in this genotyping analysis were not the same as those used in the acute temperature ramp experiments described above; however, they were collected from the same sites in the same year and are therefore considered representative of *Symbiodinium* communities hosted by *A. poculata* at the particular VA and RI sites discussed here.

STATISTICAL ANALYSES

Astrangia poculata metabolic rates (R and P_{gross}) were analyzed using two approaches. First, holobiont, skeleton, and corrected metabolic rates were compared among temperature,

symbiotic status, and origin using a repeated measures ANOVA (aov function in R v3.4.0; R Core Team 2017), with genotype included as the repeated measure term to account for natural variation between genotype and temperature, and fixed factors of symbiotic status and origin. When main effects were detected, Tukey's honestly significant difference (HSD) *post hoc* analyses were used to identify significant paired contrasts (lsmeans function in R v3.4.0; R Core Team 2017). The ANOVA results for R_{corr} and P_{gross} are included in Tables 1 and 2, respectively, and the summary of all other statistical analyses for the metabolic rates is included in Tables S1-S10. Data from both heat and cold ramps were combined for this analysis, after randomly sampling half of the 18°C measurements in order to maintain the same n for each temperature.

Second, the entire TPC of each individual was natural log-transformed and fitted to the Sharpe-Schoolfield equation in order to quantify the thermal optimum (T_{opt}) for each individual. Following the methods outlined in Padfield et al. (2016), the best fit to each TPC was determined by nonlinear least squares regression using the 'nlsLM' function in the 'minpack.lm' package (Elzhov et al., 2009), implemented in R v3.4.0 (R Core Team, 2017). The Sharpe-Schoolfield equation yields the maximum metabolic rate at the optimum temperature, T_{opt} (Padfield et al., 2016), which was estimated for each individual. The uncertainty in the Sharpe-Schoolfield fit and parameters, including T_{opt}, was estimated using parametric bootstrapping following the approach outlined by Thomas et al. (2012). This approach was found to be most appropriate for this dataset because the TPCs measured here did not capture many points past the optimum temperature. T_{opt} was compared between origin and symbiotic state using a fixed-effects ANOVA (aov function in R v3.4.0; R Core Team 2017), with fixed effects of origin and color. Because we were unable to measure many points past the thermal optimum of the population, it was difficult to confidently estimate T_{opt} for every individual; therefore, outliers (estimates of $T_{opt} < 0$) were excluded from the analysis.

F_v/F_m was analyzed as above using a repeated-measures ANOVA and Tukey's HSD *post hoc* analyses when main effects were detected. The three replicate measurements per individual at each temperature were averaged before analysis and heat and cold ramps were combined with random sampling of half of the 18°C measurements. Holobiont and skeleton F_v/F_m were analyzed separately.

The effects of *A. poculata* origin and color on mean red channel intensity (i.e., proxy of algal pigments) was assessed using a fixed-effects ANOVA, with origin and color included as fixed effects. This analysis was conducted separately for both holobiont and skeleton photos.

RESULTS

IN SITU THERMAL ENVIRONMENT

Overall, VA SST was higher than RI as recorded by the two NOAA buoys over the course of the time considered here (Fig. 2A). At the depth of the collection sites, this pattern was maintained for most of the time recorded. However, while RI was consistently colder than VA in the winter months, RI was warmer than VA during many of the summer months (e.g., June-August; Fig. 2A, Hobo loggers). This is likely due to the shallower depth of collection of RI corals and therefore a greater amount of time spent above the summer thermocline. The Rhode Island collection site spent 19.2% of the time recorded by *in situ* loggers at the coldest temperatures overall (between 2 and 6°C; Fig. 2B), and the coldest temperature recorded was 3.1°C (February 14, 2017 at 04:40). In contrast, the coldest temperature recorded by *in situ* loggers in VA was 7.5°C (January 25, 2017 at 03:15). The VA site spent 17.7% of the time recorded at the warmest temperatures (between 22 and 26°C), while Rhode Island spent only 0.1% of the time recorded between these same temperatures (Fig. 2B). The maximum temperatures recorded by *in situ* loggers at the VA and RI collection sites were 25.0°C (September 3, 2016 at 12:15) and 23.2°C (August 28, 2016 at 15:32), respectively.

METABOLIC THERMAL RESPONSE

I predicted that VA *A. poculata* would have higher metabolic performance than RI *A. poculata* at higher temperatures, and vice versa at cold temperatures, due to adaptation to distinct local thermal environments. Corrected dark respiration (R_{corr}) was significantly different based on origin ($p = 0.02$; Table 1); however, RI R_{corr} was greater than VA overall (Fig. 3; Tukey's HSD $p = 0.003$; Table S3). R_{corr} was also significantly higher in RI corals compared to VA corals across the majority of the temperatures measured here (Fig. 3; 6°C, $p = 0.02$, 15°C, $p = 0.03$, 18°C, $p = 0.008$, 22°C, $p < 0.0001$, and 26°C, $p = 0.0002$; Table S3). As predicted by Arrhenius kinetics (Angilletta, 2009; Schulte et al., 2011), R_{corr} was significantly affected by temperature ($p < 0.0001$; Table 1). Additionally, R_{corr} of white corals was higher than brown corals overall (Fig. 3; $p = 0.02$; Table 1; Tukey's HSD $p = 0.001$; Table S3).

Dark respiration rates of *A. poculata* holobiont and skeleton, which were used to calculate the R_{corr} rate, are shown in Figures S3 and S4, respectively. Few differences were observed between the holobiont and corrected dark respiration rates, except that within temperature, RI holobiont fragments had higher dark respiration rates than VA holobiont fragments at 29°C ($p = 0.02$) in addition to the temperatures listed above (Table S1). Additionally, white respiration exceeded brown respiration within all temperatures ($p < 0.01$ at all temperatures; Table S1). *A. poculata* skeleton dark respiration rates were only significantly affected by temperature (Fig. S3; $p < 0.0001$; Table S2).

In contrast to R_{corr}, there was no effect of origin on *A. poculata* holobiont gross photosynthesis (P_{gross}; Fig. 4; $p = 0.073$; Table 2). Holobiont P_{gross} was significantly higher in brown versus white corals overall (Fig. 4; $p < 0.001$; Table 2; Tukey's HSD $p < 0.001$; Table S4). P_{gross} was also significantly affected by temperature ($p < 0.001$; Table 2). There were interactive effects of color and temperature on P_{gross} ($p = 0.008$; Table 2), and within temperatures, P_{gross} was greater in brown than white corals at all temperatures except 9°C (Table S4).

Holobiont P_{gross} is presented here because many of the skeleton P_{gross} measurements were negative (i.e., no gross production; Fig. S6) and therefore did not produce a reasonable measure of P_{corr} (Fig. S5). Negative P_{gross} values result from elevated respiration measured in the light compared to the dark. The negative P_{gross} rates measured here are likely a result of the white corals, and at some temperatures brown corals, performing little measurable photosynthesis, therefore indicating random variation in light and dark respiration and/or lack of instrument sensitivity instead of evidence of light-enhanced respiration. P_{corr} was significantly affected by color ($p < 0.0001$), temperature ($p = 0.003$) and the interaction of the two ($p < 0.02$; Table S6). As with dark respiration, skeleton P_{gross} was significantly affected by temperature only ($p = 0.01$; Table S5).

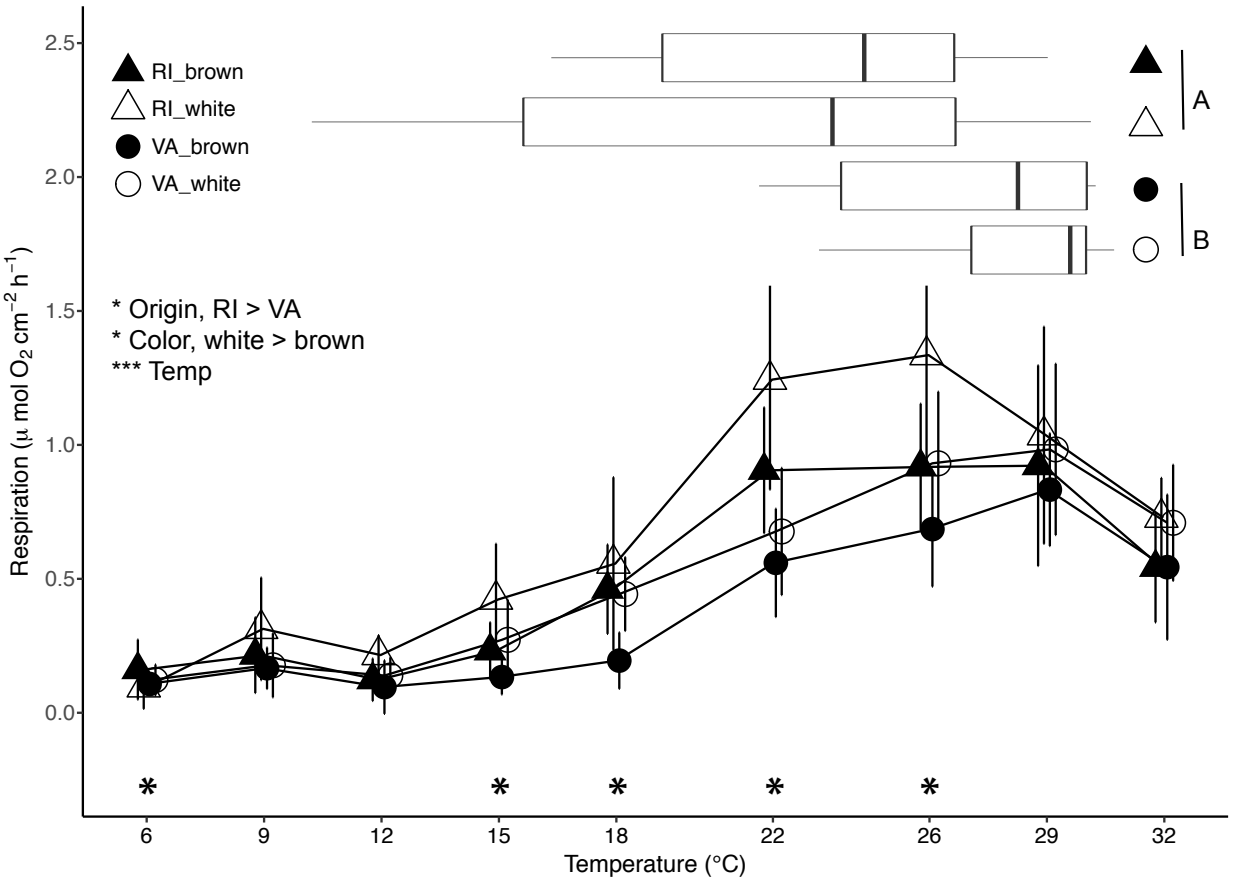

Fig. 3. ***Astrangia poculata*** **corrected dark respiration thermal performance curve and estimated T_{opt}.** Thermal performance curves (TPC) of dark respiration rates of brown (dark symbols) and white (open symbols) RI (triangles) and VA (circles) corals corrected for rates of skeleton-associated endolithic organisms between 6 and 32°C and the T_{opt} estimates from the same data (box plots). Origin, color, and temperature had a significant effect on corrected dark respiration rates (* = $p < 0.05$, *** = $p < 0.0001$). Asterisks above the x-axis indicate temperatures at which significant ($p < 0.05$) within-temperature differences between VA and RI corrected respiration were detected, with RI greater than VA in all cases. A and B designations next to the boxplots indicate significant differences in T_{opt} by origin. Each data point of the TPC is an average of n = 8 distinct individuals and error bars are 95% confidence intervals.

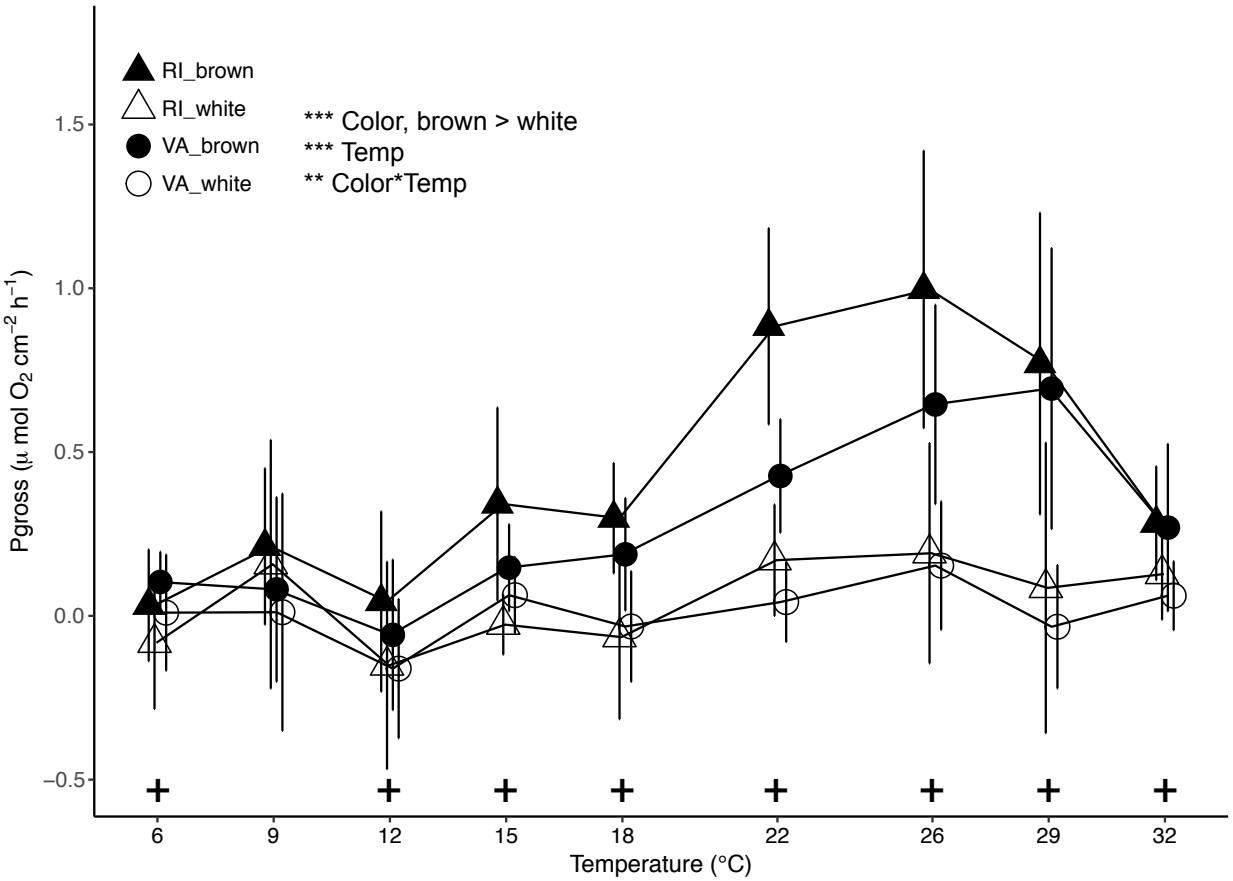

Fig. 4. ***Astrangia poculata*** **holobiont gross photosynthesis.** Gross photosynthesis (net photosynthesis – dark respiration) rates of brown (dark symbols) and white (open symbols) RI (triangles) and VA (circles) coral holobionts between 6 and 32°C. Color, temperature, and color*temperature all had a significant effect on gross photosynthesis rates (** = $p < 0.01$, *** = $p < 0.0001$). Plus signs above the x-axis indicate temperatures at which significant ($p < 0.05$) within-temperature differences between brown and white gross photosynthesis were detected, with brown greater than white in all cases. Each data point is an average of n = 8 distinct individuals and error bars are 95% confidence intervals.

Table 1. Corrected dark respiration ANOVA summary

Model: Rdark ~ Origin*Color*Temp + Error(Genotype/Temp)

Between-Subjects

Factor	Df	Sum_Sq	Mean_Sq	F_value	Pr(>F)	
Origin	1	1.56	1.56	6.36	**0.018**	*
Color	1	1.50	1.50	6.12	**0.020**	*
Origin*Color	1	0.0240	0.0244	0.099	0.75	
Residuals	28	6.88	0.246			

Within-Subjects

Factor	Df	Sum_Sq	Mean_Sq	F_value	Pr(>F)	
Temp	1	22.8	22.8	169.2	**<0.0001**	***
Origin*Temp	1	0.080	0.080	0.594	0.45	**
Color*Temp	1	0.35	0.35	2.59	0.12	
Origin*Color*Temp	1	0.008	0.008	0.058	0.81	
Residuals	28	3.78	0.135			

Table 2. Holobiont gross photosynthesis ANOVA summary

Model: Pgross ~ Origin*Color*Temp + Error(Genotype/Temp)

Between-Subjects

Factor	Df	Sum_Sq	Mean_Sq	F_value	Pr(>F)	
Origin	1	0.61	0.61	3.46	0.073	
Color	1	7.57	7.57	42.96	**<0.0001**	***
Origin*Color	1	0.26	0.26	1.45	0.24	
Residuals	28	4.93	0.18			

Within-Subjects

Factor	Df	Sum_Sq	Mean_Sq	F_value	Pr(>F)	
Temp	1	4.64	4.64	21.6	**<0.0001**	***
Origin*Temp	1	0.11	0.11	0.489	0.49	
Color*Temp	1	1.75	1.75	8.17	**0.0080**	**
Origin*Color*Temp	1	0	0	0.001	0.98	
Residuals	28	6.001	0.22			

OPTIMUM TEMPERATURE DIFFERS BETWEEN VA AND RI

The experiments described here did not capture the full decline in metabolic rate to a critical thermal maximum (CT_{max}) that is expected on the deactivation side of a thermal performance curve (see Figs 3 and 4; Angilletta Jr et al., 2002; Angilletta, 2009; Huey and Kingsolver, 1989; Huey and Kingsolver, 1993; Huey and Stevenson, 1979). Because we did not measure many points past the thermal optimum of the two populations, we were unable to fit the Sharpe-Schoolfield equation to obtain a reasonable estimate of thermal optimum (T_{opt}) for every individual included in this study. Individuals with negative estimates (n = 1 each for VA-brown, VA-white, and RI-brown corals) and two individuals for which T_{opt} could not be estimated (both RI-white corals) were removed from the analysis. Considering only the individuals for which a reasonable estimate was obtained (n=7 VA-brown, VA-white, RI-brown and n=6 VA-white), the average T_{opt} of each population was 26.8°C (±3.7 s.d.) for VA-brown, 28.2°C (±2.7) for VA-white, 23.0°C (±5.2) for RI-brown, and 21.3°C (±7.9) RI-white. T_{opt} was significantly different across origin (Fig. 3; $p = 0.0134$; Table S9), but not color ($p = 0.9699$; Table S9), with VA T_{opt} higher than RI (Fig. 3; Tukey's HSD $p = 0.0125$; Table S9).

EFFECTS OF TEMPERATURE ON F_V/F_M OF *SYMBIODINIUM PSYGMOPHILUM*

The effect of temperature was observed not only in the metabolic rates of *Astrangia poculata,* but also in the photochemical efficiency (F_v/F_m) of the coral holobiont (Fig. 5; $p=0.001$; Table S7). F_v/F_m was highest at 18°C and significantly different from all other temperatures measured (Tukey's HSD, $p<0.001$). F_v/F_m was also greater in brown fragments than white fragments overall (Tukey's HSD, $p<0.001$; Table S7), and an interaction between temperature and symbiotic status was observed ($p=0.001$; Table S7). This pattern was maintained at all temperatures measured except for 32°C, at which point F_v/F_m of brown and white *A. poculata* fragments converged, due to the higher F_v/F_m of white corals at the warmer temperatures as compared to the cold temperatures (Fig. 5; Table S7).

F_v/F_m measurements were also different in the skeletons, with VA skeleton F_v/F_m lower than RI skeleton fragments overall (Tukey's HSD, $p=0.002$; Fig. S7; $p<0.001$; Table S8). Even with the tissue and associated symbionts removed, skeleton F_v/F_m was significantly affected by the original color of the fragment ($p=0.04$; Table S8). Lastly, interactive effects of origin and

color (p=0.031) as well as origin, color, and temperature (p=0.014; Table S8) were observed in skeleton F_v/F_m.

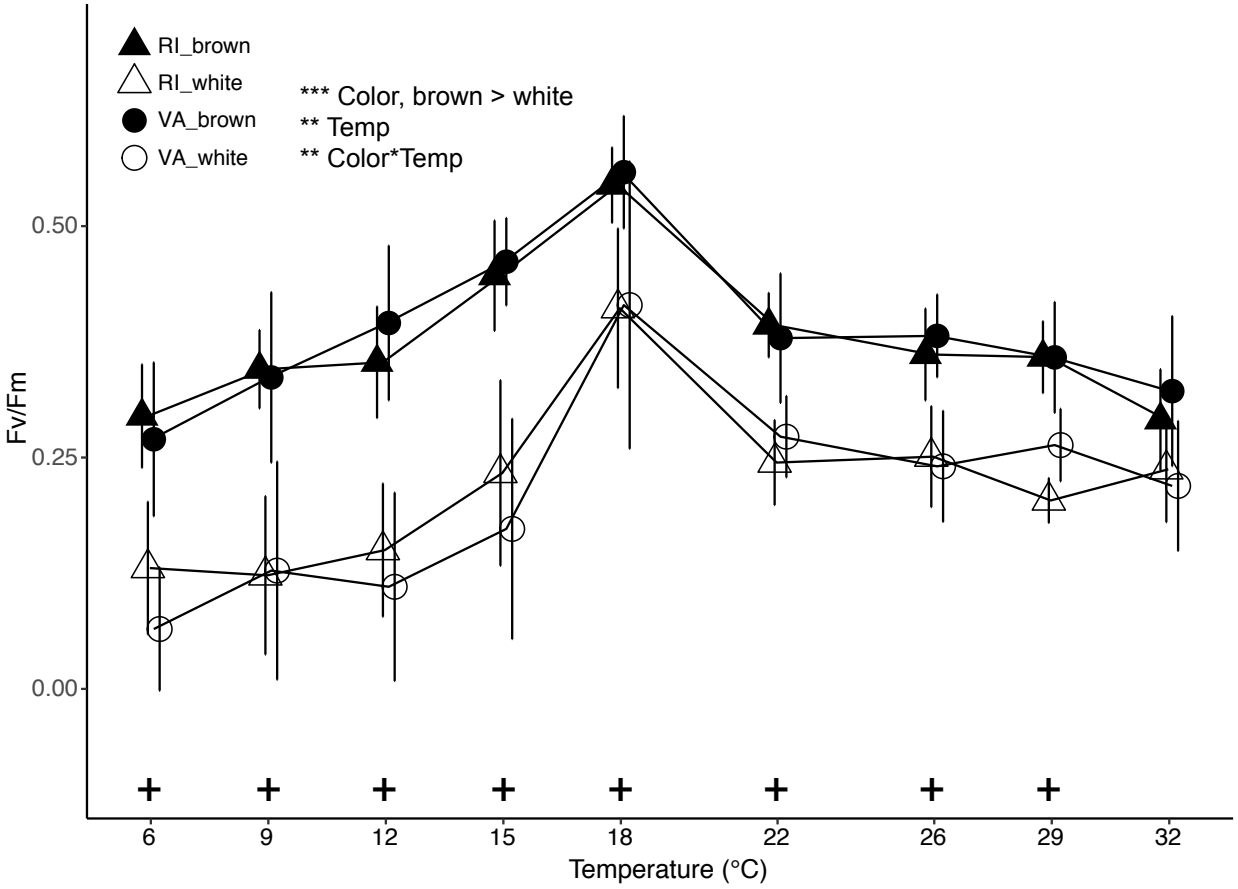

Fig. 5. ***Symbiodinium psygmophilum*** **photochemical efficiency.** Photochemical efficiency of brown (dark symbols) and white (open symbols) RI (triangles) and VA (circles) coral holobionts between 6 and 32°C. Color, temperature, and color*temperature all had a significant effect on photochemical efficiency (** = $p < 0.01$, *** = $p < 0.0001$). Plus signs above the x-axis indicate temperatures at which significant ($p < 0.05$) within-temperature differences between brown and white photochemical efficiency were detected, with brown greater than white in all cases. Each data point is an average of n = 8 distinct individuals, and each individual was measured in triplicate at all temperatures. Error bars are 95% confidence intervals.

ALGAL PIGMENT CONCENTRATIONS ARE DIFFERENT BETWEEN *A. POCULATA* POPULATIONS

Photos taken before beginning the thermal ramp experiments show that RI holobiont fragments had significantly more algal pigments than VA holobiont fragments (Fig. S8A; Tukey's HSD, $p = 0.003$; Table S10; $p = 0.00296$). As expected, holobiont brown corals had significantly more algal pigments than white corals (Fig. S8A; Tukey's HSD, $p < 0.0001$; Table S10; $p < 0.001$).

As with the holobiont fragments, RI skeleton fragments had significantly greater algal pigment density than VA skeleton (Fig. S8B; Tukey's HSD, $p < 0.001$; Table S10; $p < 0.001$). This pattern was maintained within both brown and white corals (Fig. S8B; Tukey's HSD, brown: $p = 0.026$, white: $p < 0.001$; Table S10).

RI AND VA BOTH ASSOCIATE WITH *SYMBIODINIUM PSYGMOPHILUM*

A BLASTn search against the GenBank (NCBI) database revealed that the four OTUs from the three VA and two RI individuals that passed the filtering steps of the DADA2 analysis had at least 99% similarity to *Symbiodinium psygmophilum* (accession # LK934671.1). This symbiont species has been previously shown to be the exclusive symbiotic partner of *Astrangia poculata* (LaJeunesse et al., 2012; Thornhill et al., 2008).

DISCUSSION

COUNTERGRADIENT VARIATION BETWEEN POPULATIONS IN RESPIRATION RATE

Local adaptation in thermal physiology resulting from environmentally driven selection along a species' range should lead to population-specific differences in thermal performance (Angilletta, 2009). The strongest evidence observed in this study suggesting adaptation to local thermal environments are the consistently higher dark respiration rates (i.e., metabolic activity) in Rhode Island versus Virginia *Astrangia poculata* across a variety of temperatures (6, 15, 18, 22, and 26°C; Fig. 3; Table S3). Notably, Rhode Island corals experienced the coldest temperatures recorded by the *in situ* loggers, with almost 20% of the time recorded between 2 and 6°C (Fig. 2B) and a minimum temperature of 3.1°C. In contrast, Virginia corals did not experience temperatures below 7.5°C over the time recorded. While the temperature data presented here only spans January 2016 through November 2017, the long-term pattern of Rhode Island experiencing the coldest *in situ* temperatures annually is likely consistent when considering the NOAA buoy surface temperature data at the sites (Fig. 2A). Because Rhode Island is the only site that experiences temperatures as cold as 6°C, the dark respiration data measured here suggests that RI corals are able to maintain metabolic compensation, and therefore remain active and feeding (Howe and Marshall, 2001; Jacques, 1983) at colder temperatures than VA corals. The ability of *A. poculata* metabolic rates to acclimate to a wide range of temperatures and remain active at temperatures as cold as 6.5°C has previously been established in the Narragansett Bay, RI population (Jacques, 1983); however, this finding provides evidence of local adaptation, specifically in performance at cold temperatures, of these two *Astrangia poculata* populations.

The pattern observed here, in which the cold population (RI) exhibited greater metabolic rates than the warm population (VA), is consistent with countergradient variation (Angilletta, 2009; Conover and Schultz, 1995; Gardiner et al., 2010; Sanford and Kelly, 2011), wherein the cold population outperforms the warm population at all temperatures. A recent example of countergradient variation was presented by Gardiner et al. (2010), in which aerobic scope of several species of tropical coral reef fish was greater overall in higher latitude (colder) populations as compared to lower-latitude (warmer) populations. This phenomenon is named

because the genetic and environmental effects on performance counter each other (Angilletta, 2009; Conover and Schultz, 1995; Gardiner et al., 2010).

The metabolic cold adaptation (MCA) hypothesis provides one explanation for countergradient variation, and outlines that populations from colder environments maintain mass-specific metabolic rates greater than counterparts of the same species from warmer regions as an evolutionary adaptation to compensate for lower biochemical reaction rates (Addo‐Bediako et al., 2002; Clarke, 1993; Pörtner et al., 1998; Thiel et al., 1996). Pörtner et al. (2000) link the MCA to a model of thermal tolerance from an energetic point of view, outlining that the thermal limits of an organism are the temperatures at which aerobic respiration can no longer meet energetic demands. In this model, low temperatures inhibit mitochondrial production of ATP, while high temperatures prevent ventilation/circulation from supplying mitochondria with sufficient oxygen (Angilletta, 2009; Pörtner et al., 2000). Under this model, changes in mitochondrial mechanisms may determine an organism's tolerance to a particular thermal environment, leading to differences in base metabolic rates between populations adapted to distinct temperature environments (Guderley, 2004; Pörtner et al., 1998; Pörtner et al., 2000; Sommer and Pörtner, 2002). For example, mitochondrial proliferation in a cold-adapted population can promote increased aerobic capacity and a downward shift in the critical thermal minimum (CT_{min}) as compared to a warm-adapted population (Angilletta, 2009; Pörtner et al., 1998; Sommer and Pörtner, 2002). However, the consequence of this increased capacity of aerobic energy production at colder temperatures is elevated metabolic rates overall in the cold population, resulting from the cost of synthesis and maintenance of additional mitochondria, driving the elevated baseline rates of mitochondrial oxygen consumption (Angilletta, 2009; Pörtner et al., 1998; Sommer and Pörtner, 2002). Sommer and Pörtner (2002) provide evidence for this theory in a marine invertebrate, reporting 2.4 times greater mitochondrial volume density in muscle tissue and corresponding increased metabolic demands in a cold-adapted sub-Arctic population of lugworms (*Arenicola marina*) compared to a warm-adapted temperate population of the same species (Pörtner et al., 1998; Sommer and Pörtner, 2002). Although changes in mitochondrial capacities were not explored here, the hypothesis outlined by Pörtner and colleagues provides one potential explanation for the greater overall dark respiration rates in the RI population of *A. poculata* compared to the VA population (Fig. 3). Namely, RI corals may have adapted to their colder thermal environment via mitochondrial proliferation, therefore

resulting in higher oxygen consumption rates overall compared to VA corals. In the future, it would be interesting to examine potential differences in mitochondrial density in *A. poculata* between RI and VA corals.

ELEVATED THERMAL OPTIMA IN VA CORALS

Although population differences in dark respiration were observed at 6°C and in the middle of the temperature range (Fig. 3), there was no evidence of population differences in corrected respiration at the warmest temperatures measured here (29 and 32°C). This lack of origin effect at 29 and 32°C appears to result from a decline in RI-white coral respiration after 26°C to match rates similar to the VA corals (Fig. 3).

However, we did find evidence of population differences in thermal optima (T_{opt}; Fig. 3), with T_{opt} estimates of the VA population 3.76°C (brown) and 6.88°C (white) higher than the RI population. While we acknowledge some limitations to these analyses (see below), the estimates of T_{opt} obtained here follow the convention of the warmer population (VA) being adapted to its thermal environment and exhibiting a greater thermal optimum (Angilletta, 2009). Therefore, while RI corals had higher respiration rates overall (evidence of countergradient variation), the VA TPCs appear to be shifted whereby VA corals have a warmer optimum temperature. This population difference in T_{opt} is the second line of evidence supporting adaptation to the local thermal environment in VA and RI *A. poculata*. Just as RI corals experienced colder temperatures *in situ* and performed better at 6°C, VA corals spent substantially more time at warmer temperatures (Fig. 2B), hence the differences in T_{opt} may indicate a greater upper thermal limit of the VA population. We acknowledge that because the entire thermal performance curve (i.e., the full decline in metabolic rate to CT_{max}) was not captured in these experiments, additional work is needed to obtain a more confident estimate of thermal optimum for these two populations. Specifically, the experiments described here should be expanded to include temperatures above 32°C to increase confidence in the validity of the T_{opt} estimates.

SIMILAR PHOTOSYNTHESIS AND F_V/F_M RESPONSES BETWEEN ORIGINS

Brown colonies housing *Symbiodinium psygmophilum* were able to maintain P_{gross} rates greater than white colonies at every temperature measured here except 9°C (Fig. 4), which was

to be expected based on the contribution of *S. psygmophilum* to the holobiont energy budget. Despite maintaining rates greater than white colonies, rates of P_{gross} in brown corals overall were low, and indeed the 95% confidence intervals of brown P_{gross} overlapped with 0 μmol O_2 cm^2 h^{-1} at the majority of temperatures for RI (6, 9, 12, 15, 18°C) and two temperatures for VA (9, 12°C) corals. With such negligible rates of P_{gross}, *S. psygmophilum* likely only provides significant photosynthetic by-products (i.e., glucose; Burriesci et al., 2012) to the host at temperatures above 22°C (Fig. 4). Therefore, for the majority of the year (Fig. 2) *A. poculata* likely depends primarily on heterotrophic inputs to meet its metabolic requirements. This finding is similar to that of Jacques (1983), who concluded that symbiont photosynthesis was only sufficient to provide a growth benefit to RI *A. poculata* above 15°C, or for 4 months of the year (also see Dimond and Carrington, 2007).

In terms of photochemical efficiencies, similar values (~0.5) for F_v/F_m were previously obtained from corals collected from the same RI site and maintained at 18°C (Burmester et al., 2017). This supports the convention that the *A. poculata* F_v/F_m measured here at 18°C indicates healthy photochemical efficiency of these populations at this acclimation temperature. However, the significant decreases in F_v/F_m observed at all other temperatures for both VA and RI corals (Fig. 5; Table S7) are more difficult to interpret. On one hand, decreases in F_v/F_m could indicate a stress response of *S. psygmophilum* (Falkowski and Raven, 2007; Fitt et al., 2001). However, as both RI and VA *A. poculata* regularly experience a range of temperatures in addition to 18°C in the field (Fig. 2), it is unlikely that temperatures close to 18°C would induce photochemical stress on *S. psygmophilum in situ*. Instead, it is more likely that this trend is consistent with acclimation of the photochemical efficiency of *S. psygmophilum* to the common garden aquarium holding conditions (18°C; Fig. 5).

LONG-TERM ACCLIMATIZATION AND/OR DEVELOPMENTAL EFFECTS

A significant effect of origin in a common garden experiment, such as that observed in dark respiration rates here (Fig. 3), is usually attributed to potential genotype (i.e., adaptive) effects (DeWitt and Scheiner, 2004; Sanford and Kelly, 2011; Schluter, 2000). However, significant origin effects are not exclusive of other influences, such as long-term acclimatization and/or epigenetic drivers. Marine organisms exhibit phenotypic plasticity (i.e., long-term physiological acclimatization) in response to environmental variation, which mimic local

adaptation when no genetic effects are present and can be retained even after acclimation to common garden conditions (Kawecki and Ebert, 2004; Sanford and Kelly, 2011). Indeed, prior exposure of the west-facing side of the tropical coral *Coelastrea aspera* to higher solar radiation has been shown to confer tolerance to future exposure to elevated temperature and solar radiation (Brown and Dunne, 2008), and this 'memory' can last up to 10 years (Brown et al., 2015). It is therefore possible that the adaptive signature in dark respiration rates observed here could be attributed to phenotypic plasticity resulting from long-term acclimatization of *A. poculata* to the respective VA and RI thermal environments.

In addition to the effects of long-term acclimatization, the elevated dark respiration rates in RI corals could be the result of persistent maternal effects and/or epigenetic acclimatization. Little is known about these processes in the marine environment and particularly in corals; however, recent work has demonstrated that both maternal effects and epigenetic acclimatization play an important role in the sea (e.g., Marshall, 2008), particularly in the response of tropical corals to environmental change. For example, the parental temperature and pCO_2 environment has been shown to directly influence larvae size and metabolic rate in the tropical coral *Pocillopora damicornis* (Putnam and Gates, 2015). In addition to maternal effects, *P. damicornis* also demonstrated rapid induction of DNA methylation as a response to elevated pCO_2 conditions (Putnam et al., 2016). In order to completely remove the effect of the maternal environment, it would be necessary to rear *A. poculata* for two or more generations under common garden conditions in the laboratory (Sanford and Kelly, 2011; Torda et al., 2017), a process made impractical by both time and resource constraints in this case. As epigenetic mechanisms were not investigated here, we cannot dismiss the possibility that either maternal effects and/or epigenetics played a role in the adaptive signature observed.

Despite these other potential drivers of origin effects, there are several lines of evidence to support the influence of underlying genetic effects consistent with adaptation on the pattern of countergradient variation in dark respiration rates observed here. First, previous studies have shown that genetic differentiation can play a significant role in similar patterns of countergradient variation in physiological traits across a latitudinal gradient (Sanford and Kelly, 2011; Somero, 2010; Somero, 2005). Second, we did observe a signature of acclimation of photochemical efficiency to common garden conditions (see discussion above); suggesting that the acclimation time was sufficient to remove the effect of the VA and RI thermal environment

on *A. poculata*. This conclusion is further supported by Jacques (1983) finding that 3 weeks was sufficient to induce physiological acclimation in metabolic rates of *A. poculata* coral tissue, similar to the 24-day recovery and acclimation period provided here. Third, the large geographic scale covered by the two populations considered supports a pattern of adaptation resulting from isolation by distance (Sanford and Kelly, 2011; Wright, 1943). Taken together, this certainly raises the possibility that underlying genetic mechanisms may have led to the observed origin effects on *A. poculata* dark respiration rates.

CONSEQUENCE OF ELEVATED METABOLIC RATES

The positive relationship between temperature and respiration in poikilotherms (an organism whose internal temperature varies considerably, i.e., corals) can be a consequence of kinetic principles alone (Hochachka and Somero, 2002). In poikilotherms, respiration at elevated temperatures due to Arrhenius kinetics (Arrhenius, 1915) can be beneficial due to the enhanced supply of ATP, which is needed in chemical synthesis and mechanical work (Edmunds et al., 2011; Hochachka and Somero, 2002). However, the extent of this benefit depends on the organism's demands for cellular energy and the speed with which reserves can be replaced (Edmunds et al., 2011; Hochachka and Somero, 2002). These beneficial effects reverse when temperatures again decrease, as long as the temperatures did not exceed the organism's upper thermal limit (Hochachka and Somero, 2002). Extreme temperatures beyond an organism's temperature threshold (i.e., T_{opt}) result in damage to the organism's metabolic machinery and ultimately metabolic depression (Hochachka and Somero, 2002). Both extreme cold and hot temperatures have negative effects on enzymatic function and membrane structure, slowing biochemical reactions, and therefore making damage accrued beyond these extreme temperatures less readily reversed (Angilletta, 2009; Hochachka and Somero, 2002).

While the general response of metabolic rates to increasing temperature is universal, understanding the critical thresholds in corals at which the benefits of elevated metabolic rate are lost and irreversible damage is done can provide valuable insight in understanding the effects of future temperature extremes. Previous work in tropical corals found that increasing temperature caused respiratory demands to increase and the ratio of net photosynthesis to respiration (P_{net}:R) to decrease, leading to reduced capacity of the symbiotic algae to provide sugars to the host

(Coles and Jokiel, 1977). The authors suggest that this reduced capacity of the autotrophic ability of the symbiont persists until the organism either acclimates to elevated temperature, perishes, or the coral bleaches (Coles and Jokiel, 1977). Additionally, Castillo and Helmuth (2005) demonstrate that increasing temperatures result in a metabolic cost in both inshore and barrier reef populations of *Montastraea annularis* in Belize, with a sharp decline in P_{gross} and R beyond 34°C. Interestingly, metabolic rates were greater in corals from the cooler, outer reef environment compared to corals originating from the warmer inner reef (Castillo and Helmuth, 2005). While photosynthesis and respiration of tropical corals are usually impaired below 18°C (Crossland, 1984), previous work has shown that RI *A. poculata* respiration can acclimate to a wide range of temperatures (11.5 – 23°C) and even survive indefinitely at tropical temperatures of 27°C in the laboratory (Jacques, 1983). The results presented here also demonstrate the ability of *A. poculata* to withstand acute exposures to temperatures beyond what is regularly experienced in the environment (Figs 3 and 4). The ability of *A. poculata* to withstand and maintain metabolic compensation over such a wide temperature range is unique among scleractinian corals, making this species an interesting model to use in understanding thermal limits, particularly of the coral animal and symbiont independently.

IMPLICATIONS FOR FUTURE RANGE EXPANSION OF *ASTRANGIA POCULATA*

The results of this study have implications for the range of *Astrangia poculata* as SSTs continue to increase along the Mid-Atlantic US. As a result of warming temperatures, a number of both terrestrial and marine species are contracting, expanding, or shifting their ranges to track favorable conditions (Hoegh-Guldberg and Bruno, 2010; Parmesan, 2006; Parmesan and Yohe, 2003). Range shifts have been observed in many Northern-Hemisphere temperate organisms, including birds, the order Lepidoptera (butterflies and moths), and the order Odonata (dragonflies and damselflies, reviewed by Parmesan, 2006). In many instances, observed range expansions track winter temperatures, or winter cold extremes (Parmesan, 2006). Pole-ward range expansion into temperate areas has also been observed in four species of tropical coral in Japan (Yamano et al., 2011). This expansion occurred at speeds up to 14 km $year^{-1}$, and the authors suggest these types of range expansions could lead to significant modifications of temperate coastal ecosystems, which could occur at even greater speeds in regions of the world with poleward flowing currents (i.e., the Atlantic coast of the US).

The current northern range limit of *A. poculata* is Cape Cod, Massachusetts (~42°N; Dimond et al., 2012; Peters et al., 1988), and winter temperatures are believed to be the factor limiting expansion further north (Dimond et al., 2012). Dimond et al. (2012) suggest that colder temperatures north of Cape Cod correspond with unfavorable conditions for *A. poculata* growth, inability to prevent loss of surface area to competitors (i.e., macroalgae and clionid sponges), as well as a loss in benefit of associating with *S. psygmophilum*. The metabolic rate data presented here also suggests that both VA and RI populations of *A. poculata* are currently more limited by local thermal minimums rather than maxima. The estimated T_{opt} values of VA corals (VA-brown 26.8°C, VA-white 28.2°C) support this hypothesis and are greater than the observed maximum *in situ* temperature (25.0°C). It should be noted that the estimated T_{opt} values of RI corals (RI-brown 23.0°C, RI-white 21.3°C) are similar to and less than the observed maximum *in situ* temperature (23.2°C), suggesting this population may be more susceptible to future increases in temperature. However, despite measuring the acute response to temperatures more than 7°C above the current maximum temperature experienced by either population *in situ*, the full decline to CT_{max} was not observed in most individuals, suggesting both populations still exist below their upper thermal limit. The data presented here suggest that future temperature increases predicted by the Intergovernmental Panel on Climate Change (Rhein et al., 2013) will permit *A. poculata* to expand its range further north, particularly to track warming winter temperatures.

CONCLUSION

Patterns of local adaptation are proving to be more ubiquitous in the marine environment than previously believed, which has significant implications when considering population-level responses to environmental change. Here, elevated respiration rates at cold extremes along with a consistent pattern of countergradient variation suggests a signature of adaptation of VA and RI *A. poculata* to their respective thermal environments. Additionally, thermal optima (T_{opt}) estimated from dark respiration rates were higher in the warmer VA population compared to the colder RI population. The lack of a significant effect of origin on either *S. psygmophilum* P_{gross} or F_v/F_m could suggest a host-only role in the adaptive signature observed here. While we cannot definitively exclude the contribution of long-term acclimatization, maternal effects, and/or epigenetics to the observed effect of origin on dark respiration and T_{opt}, we did observe evidence of acclimation in photochemical efficiency to the common garden conditions. This evidence, taken together with previous work demonstrating the acclimation of *A. poculata* metabolic rates over similar timeframes, are suggestive that the significant origin effect observed here could be due to adaptation.

To my knowledge, this study provides the first evidence of adaptation to local thermal environments in the temperate coral *Astrangia poculata.* These findings have implications for a potential future range expansion north beyond where cold temperatures currently limit the species. As *A. poculata* is an important member of valuable Mid-Atlantic hardbottom communities, it is imperative to understand the extent of local adaptation in physiological tolerance limits to better predict how these organisms and their habitat will fare in the face of climate change.

REFERENCES

Addo‐Bediako, A., Chown, S. and Gaston, K. (2002). Metabolic cold adaptation in insects: a large‐scale perspective. *Funct Ecol* **16**, 332-338.

Angilletta Jr, M. J., Niewiarowski, P. H. and Navas, C. A. (2002). The evolution of thermal physiology in ectotherms. *J Therm Biol.* **27**, 249-268.

Angilletta, M. J. (2009). Thermal adaptation: a theoretical and empirical synthesis: Oxford University Press.

Arrhenius, S. (1915). Quantitative laws in biological chemistry. London: G. Bell.

Baker, A. and Cunning, R. (2016). Bulk gDNA extraction from coral samples. *protocols.io*.

Barshis, D. J., Stillman, J. H., Gates, R. D., Toonen, R. J., Smith, L. W. and Birkeland, C. (2010). Protein expression and genetic structure of the coral *Porites lobata* in an environmentally extreme Samoan back reef: does host genotype limit phenotypic plasticity? *Mol Ecol* **19**, 1705-1720.

Baumann, J., Davies, S. W., Aichelman, H. E. and Castillo, K. D. (2017). Coral Symbiodinium community composition across the Belize Mesoamerican Barrier Reef System is influenced by host species and thermal variability. *Microb Ecol* **75**, 1-13.

Bay, R. A. and Palumbi, S. R. (2014). Multilocus adaptation associated with heat resistance in reef-building corals. *Curr Biol* **24**, 2952-2956.

Brown, B. and Dunne, R. (2008). Solar radiation modulates bleaching and damage protection in a shallow water coral. *Mar Ecol Prog Ser.* **362**, 99-107.

Brown, B. E., Dunne, R. P., Edwards, A. J., Sweet, M. J. and Phongsuwan, N. (2015). Decadal environmental 'memory'in a reef coral? *Mar. Biol* **162**, 479-483.

Burmester, E., Finnerty, J., Kaufman, L. and Rotjan, R. (2017). Temperature and symbiosis affect lesion recovery in experimentally wounded, facultatively symbiotic temperate corals. *Mar Ecol Prog Ser.* **570**, 87-99.

Burriesci, M. S., Raab, T. K. and Pringle, J. R. (2012). Evidence that glucose is the major transferred metabolite in dinoflagellate–cnidarian symbiosis. *J. Exp. Biol.* **215**, 3467-3477.

Callahan, B. J., McMurdie, P. J., Rosen, M. J., Han, A. W., Johnson, A. J. A. and Holmes, S. P. (2016). DADA2: high-resolution sample inference from Illumina amplicon data. *Nat. Methods* **13**, 581.

Castillo, K. and Helmuth, B. (2005). Influence of thermal history on the response of *Montastraea annularis* to short-term temperature exposure. *Mar. Biol* **148**, 261-270.

Clarke, A. (1993). Seasonal acclimatization and latitudinal compensation in metabolism: do they exist? *Funct Ecol* **7**, 139-149.

Coles, S. and Jokiel, P. (1977). Effects of temperature on photosynthesis and respiration in hermatypic corals. *Mar. Biol* **43**, 209-216.

Conover, D. O., Duffy, T. A. and Hice, L. A. (2009). The covariance between genetic and environmental influences across ecological gradients. *Ann N Y Acad Sci* **1168**, 100-129.

Conover, D. O. and Schultz, E. T. (1995). Phenotypic similarity and the evolutionary significance of countergradient variation. *Trends Ecol. Evol.* **10**, 248-252.

Crossland, C. (1984). Seasonal variations in the rates of calcification and productivity in the coral *Acropora formosa* on a high-latitude reef. *Mar Ecol Prog Ser.* **15**, 135-140.

Davies, P. S. (1989). Short-term growth measurements of corals using an accurate buoyant weighing technique. *Mar. Biol* **101**, 389-395.

DeFilippo, L., Burmester, E. M., Kaufman, L. and Rotjan, R. D. (2016). Patterns of surface lesion recovery in the Northern Star Coral, *Astrangia poculata*. *J. Exp. Mar. Biol. Ecol* **481**, 15-24.

DeWitt, T. and Scheiner, S. (2004). Phenotypic variation from single genotypes. In *Phenotypic Plasticity: Functional and conceptual approaches*, eds. T. DeWitt and S. Scheiner), pp. 1-9. New York: Oxford University Press.

Dimond, J. and Carrington, E. (2007). Temporal variation in the symbiosis and growth of the temperate scleractinian coral *Astrangia poculata*. *Mar Ecol Prog Ser.* **348**, 161-172.

Dimond, J. L., Kerwin, A. H., Rotjan, R., Sharp, K., Stewart, F. J. and Thornhill, D. J. (2012). A simple temperature-based model predicts the upper latitudinal limit of the temperate coral *Astrangia poculata*. *Coral Reefs* **32**, 401-409.

Edmunds, P. J., Cumbo, V. and Fan, T.-Y. (2011). Effects of temperature on the respiration of brooded larvae from tropical reef corals. *J. Exp. Biol.* **214**, 2783-2790.

Elzhov, T. V., Mullen, K. M. and Bolker, B. (2009). minpack.lm: R interface to the Levenberg-Marquardt Nonlinear Least-Squares Algorithm Found in MINPACK. R Packag. version.

Falkowski, P. G. and Raven, J. A. (2007). Aquatic Photosynthesis (Second Edition). Princeton New Jersey: Princeton University Press.

Fitt, W. K., Brown, B. E., Warner, M. E. and Dunne, R. P. (2001). Coral bleaching: interpretation of thermal tolerance limits and thermal thresholds in tropical corals. *Coral Reefs* **20**, 51-65.

Gardiner, N. M., Munday, P. L. and Nilsson, G. E. (2010). Counter-gradient variation in respiratory performance of coral reef fishes at elevated temperatures. *PLoS One* **5**, e13299.

Guderley, H. (2004). Metabolic responses to low temperature in fish muscle. *Biol Rev* **79**, 409-427.

Hochachka, P. and Somero, G. (2002). Biochemical Adaptation: Mechanism and Process in Physiological Evolution. New York: Oxford University Press.

Hoegh-Guldberg, O. and Bruno, J. F. (2010). The impact of climate change on the world's marine ecosystems. *Science* **328**, 1523-1528.

Holcomb, M., Cohen, A. L. and McCorkle, D. C. (2012). An investigation of the calcification response of the scleractinian coral *Astrangia poculata* to elevated pCO2 and the effects of nutrients, zooxanthellae and gender. *Biogeosciences* **9**, 29-39.

Holcomb, M., McCorkle, D. C. and Cohen, A. L. (2010). Long-term effects of nutrient and CO 2 enrichment on the temperate coral *Astrangia poculata* (Ellis and Solander, 1786). *J. Exp. Mar. Biol. Ecol* **386**, 27-33.

Howe, S. A. and Marshall, A. T. (2001). Thermal compensation of metabolism in the temperate coral, *Plesiastrea versipora* (Lamarck, 1816). *J. Exp. Mar. Biol. Ecol* **259**, 231-248.

Huey, R. B. and Kingsolver, J. G. (1989). Evolution of thermal sensitivity of ectotherm performance. *Trends Ecol. Evol.* **4**, 131-135.

Huey, R. B. and Kingsolver, J. G. (1993). Evolution of resistance to high temperature in ectotherms. *Am. Nat.* **142**, S21-S46.

Huey, R. B. and Stevenson, R. (1979). Integrating thermal physiology and ecology of ectotherms: a discussion of approaches. *Am Zool* **19**, 357-366.

Jacques, T. G. M., N.; Pilson, M.E.Q. (1983). Experimental ecology of the temperate scleractinian coral *Astrangia danae* II. Effect of temperature, light intensity and symbiosis with zooxanthellae on metabolic rate and calcification. *Mar. Biol* **76**, 135-148.

Jacques, T. G. P., M.E.Q. (1980). Experimental Ecology of the Temperate Scleractinian Coral *Astrangia danae* I. Partition of Respiration, Photosynthesis, and Calcification Between Host and Symbionts. *Mar. Biol* **60**, 167-178.

Kawecki, T. J. and Ebert, D. (2004). Conceptual issues in local adaptation. *Ecol Lett* **7**, 1225-1241.

Kenkel, C., Goodbody‐Gringley, G., Caillaud, D., Davies, S., Bartels, E. and Matz, M. (2013). Evidence for a host role in thermotolerance divergence between populations of the mustard hill coral (*Porites astreoides*) from different reef environments. *Mol Ecol* **22**, 4335-4348.

LaJeunesse, T. C., Parkinson, J. E. and Reimer, J. D. (2012). A genetics‐based description of *Symbiodinium minutum* sp. nov. and *S. psygmophilum* sp. nov.(Dinophyceae), two dinoflagellates symbiotic with cnidaria. *J Phycol* **48**, 1380-1391.

Marshall, D. J. (2008). Transgenerational plasticity in the sea: Context‐dependent maternal effects across the life history. *Ecology* **89**, 418-427.

Olito, C., White, C. R., Marshall, D. J. and Barneche, D. R. (2017). Estimating monotonic rates from biological data using local linear regression. *J. Exp. Biol.* **220**, 759-764.

Padfield, D., Yvon‐Durocher, G., Buckling, A., Jennings, S. and Yvon‐Durocher, G. (2016). Rapid evolution of metabolic traits explains thermal adaptation in phytoplankton. *Ecol Lett* **19**, 133-142.

Palumbi, S. R., Barshis, D. J., Traylor-Knowles, N. and Bay, R. A. (2014). Mechanisms of reef coral resistance to future climate change. *Science* **344**, 895-898.

Parmesan, C. (2006). Ecological and evolutionary responses to recent climate change. *Annu. Rev. Ecol. Evol. Syst.* **37**, 637-669.

Parmesan, C. and Yohe, G. (2003). A globally coherent fingerprint of climate change impacts across natural systems. *Nature* **421**, 37.

Peters, E. C., Cairns, S. D., Pilson, M. E., Wells, J. W., Jaap, W. C., Lang, J. C., Vasleski, C. and St Pierre Gollahon, L. (1988). Nomenclature and biology of *Astrangia poculata* (= *A. danae*,= *A. astreiformis*)(Cnidaria: Anthozoa). *Proc Biol Soc Wash* **101**, 234-250.

Pörtner, H.-O., Hardewig, I., Sartoris, F. and Van Dijk, P. (1998). Energetic aspects of cold adaptation: critical temperatures in metabolic, ionic and acid-base regulation. *Cold Ocean Physiology* **66**, 88-120.

Pörtner, H.-O., Van Dijk, P., Hardewig, I. and Sommer, A. (2000). Levels of metabolic cold adaptation: tradeoffs in eurythermal and stenothermal ectotherms. In *Antarctic Ecosystems: models for wider ecological understanding*, eds. W. Davison and C. H. Williams), pp. 109-122. Christchurch New Zealand: Caxton Press.

Putnam, H. M., Davidson, J. M. and Gates, R. D. (2016). Ocean acidification influences host DNA methylation and phenotypic plasticity in environmentally susceptible corals. *Evol Appl.* **9**, 1165-1178.

Putnam, H. M. and Gates, R. D. (2015). Preconditioning in the reef-building coral *Pocillopora damicornis* and the potential for trans-generational acclimatization in coral larvae under future climate change conditions. *J. Exp. Biol.* **218**, 2365-2372.

R Core Team. (2017). R: A language and environment for statistical computing. Vienna, Austria.

Rhein, M., Rintoul, S., Aoki, S., Campos, E., Chambers, D., Feely, R., Gulev, S., Johnson, G., Josey, S. and Kostianoy, A. (2013). Climate Change 2013: The Physical Science Basis.

Contribution of Working Group I to the 5th Assessment Report of the IPCC: Cambridge: Cambridge University Press.

Ries, J. B. (2011). A physicochemical framework for interpreting the biological calcification response to CO2-induced ocean acidification. *Geochim. Cosmochim. Acta* **75**, 4053-4064.

Sanford, E. and Kelly, M. W. (2011). Local adaptation in marine invertebrates. *Ann Rev Mar Sci.* **3**, 509-535.

Schindelin, J., Rueden, C. T., Hiner, M. C. and Eliceiri, K. W. (2015). The ImageJ ecosystem: An open platform for biomedical image analysis. *Mol Reprod Dev* **82**, 518-529.

Schluter, D. (2000). The Ecology of Adaptive Radiation. Oxford: Oxford University Press.

Schulte, P. M., Healy, T. M. and Fangue, N. A. (2011). Thermal performance curves, phenotypic plasticity, and the time scales of temperature exposure. *Integr. Comp. Biol* **51**, 691-702.

Somero, G. (2010). The physiology of climate change: how potentials for acclimatization and genetic adaptation will determine 'winners' and 'losers'. *J. Exp. Biol.* **213**, 912-920.

Somero, G. N. (2005). Linking biogeography to physiology: evolutionary and acclimatory adjustments of thermal limits. *Front Zool* **2**, 1.

Sommer, A. and Pörtner, H.-O. (2002). Metabolic cold adaptation in the lugworm *Arenicola marina*: comparison of a North Sea and a White Sea population. *Mar Ecol Prog Ser.* **240**, 171-182.

Tepolt, C. K. and Somero, G. N. (2014). Master of all trades: thermal acclimation and adaptation of cardiac function in a broadly distributed marine invasive species, the European green crab, *Carcinus maenas*. *J. Exp. Biol.* **217**, 1129-1138.

Thiel, H., Pörtner, H.-O. and Arntz, W. (1996). Marine life at low temperatures-a comparison of polar and deep-sea characteristics. In *Deep-sea and Extreme Shallow-water Habitats: Affinities and Adaptations* vol. 11 eds. F. Uiblein J. Ott and M. Stachowitsch), pp. 183-219. Vienna: Austrian Academy of Sciences.

Thomas, M. K., Kremer, C. T., Klausmeier, C. A. and Litchman, E. (2012). A global pattern of thermal adaptation in marine phytoplankton. *Science* **338**, 1085-1088.

Thornhill, D. J., Kemp, D. W., Bruns, B. U., Fitt, W. K. and Schmidt, G. W. (2008). Correspondence between Cold Tolerance and Temperate Biogeography in a Western Atlantic *Symbiodinium* (Dinophyta) Lineage(1). *J Phycol* **44**, 1126-35.

Torda, G., Donelson, J. M., Aranda, M., Barshis, D. J., Bay, L., Berumen, M. L., Bourne, D. G., Cantin, N., Foret, S. and Matz, M. (2017). Rapid adaptive responses to climate change in corals. *Nat. Clim. Change.* **7**, 627.

Veron, J. E. (2000). Corals of the World, vol. 1–3. Townsville: Australian Institute of Marine Science.

Warner, M., Fitt, W. and Schmidt, G. (1996). The effects of elevated temperature on the photosynthetic efficiency of zooxanthellae in hospite from four different species of reef coral: a novel approach. *Plant Cell Environ* **19**, 291-299.

Winters, G., Holzman, R., Blekhman, A., Beer, S. and Loya, Y. (2009). Photographic assessment of coral chlorophyll contents: implications for ecophysiological studies and coral monitoring. *J. Exp. Mar. Biol. Ecol* **380**, 25-35.

Wright, S. (1943). Isolation by distance. *Genetics* **28**, 114-138.

Yamano, H., Sugihara, K. and Nomura, K. (2011). Rapid poleward range expansion of tropical reef corals in response to rising sea surface temperatures. *Geophys. Res. Lett.* **38**.

APPENDIX A

SUPPLEMENTARY FIGURES

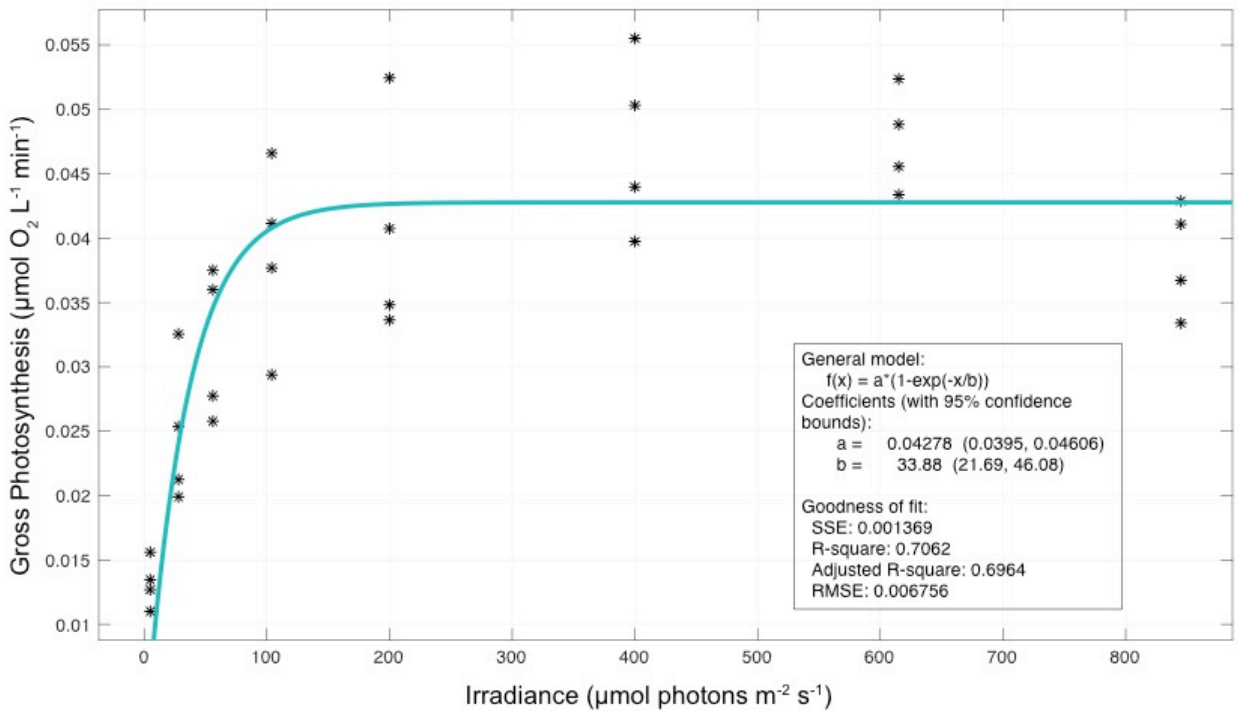

Fig. S1. Photosynthesis vs. Irradiance curve of Virginia *Astrangia poculata*. *A. poculata* gross photosynthesis measured at 8 irradiance values between 5 and 845µmol photons $m^{-2}s^{-1}$. Each data point represents gross photosynthesis of one VA *A. poculata* individual, and 4 VA brown individuals were measured in total. Inset shows goodness of fit statistics and parameter estimates from the exponential least squares best fit, where a = maximum rate of light saturated photosynthesis (P_{max}) and b = the irradiance required to saturate photosynthesis (E_k). This curve was used to pick 400µmol photons $m^{-2}s^{-1}$ as the light intensity used in the thermal ramp experiments.

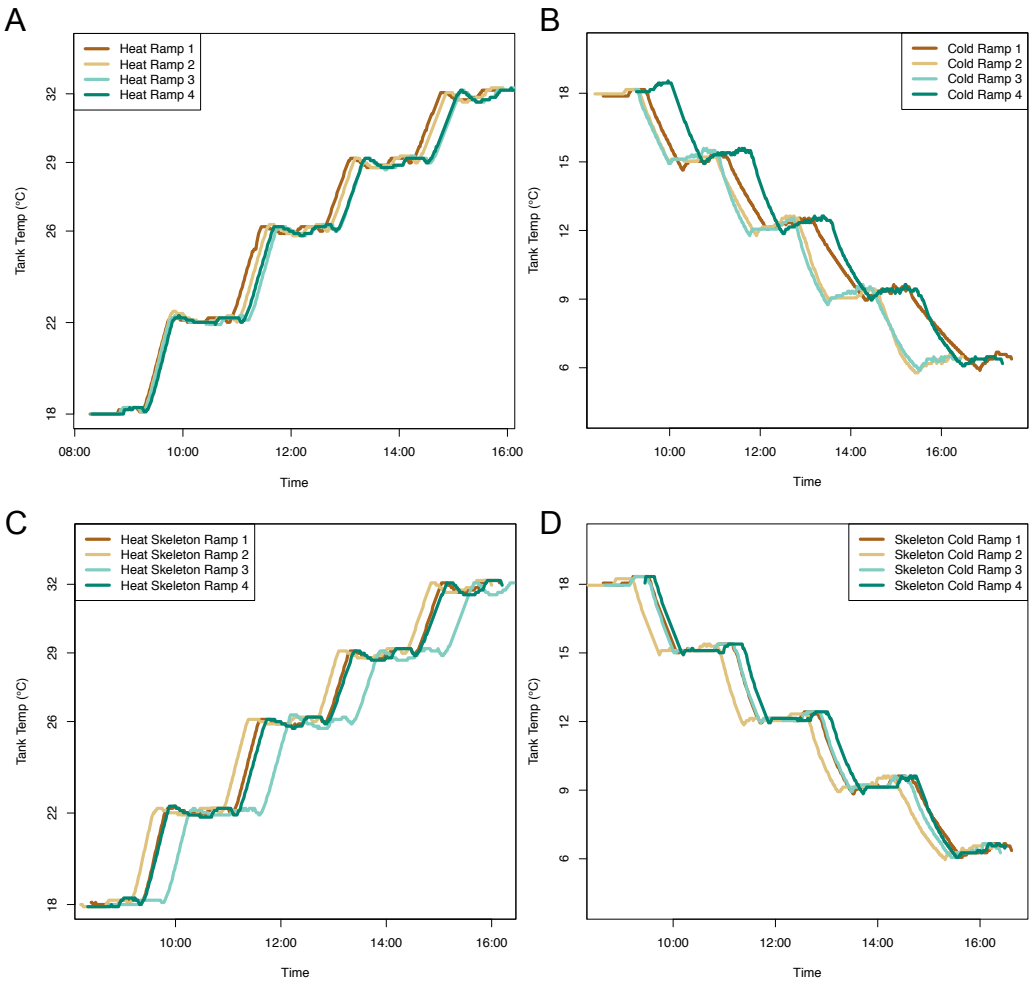

Fig. S2. Temperature conditions and timing of the heat ramps (panel A), cold ramps (panel B), heat skeleton ramps (panel C), and cold skeleton ramps (panel D). Temperature was recorded every minute by a Hobo pendant temperature logger (Onset Computer Corp.) in all ramp experiments.

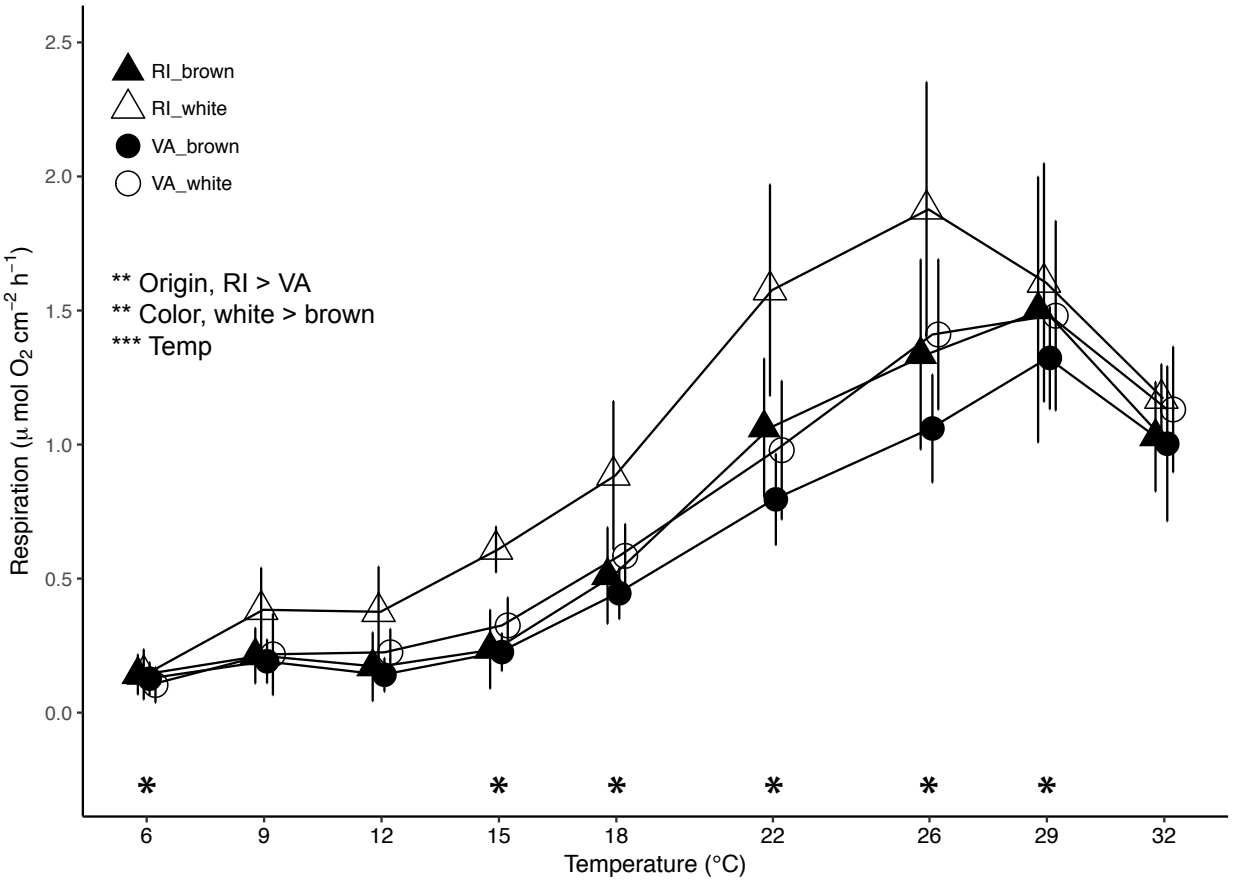

Fig. S3. ***Astrangia poculata*** **holobiont dark respiration.** Dark respiration rates of brown (dark symbols) and white (open symbols) RI (triangles) and VA (circles) coral holobionts between 6 and 32°C. Origin, color, and temperature had a significant effect on holobiont dark respiration rates (** = $p < 0.01$; *** = $p < 0.0001$). Asterisks above the x-axis indicate temperatures at which significant ($p < 0.05$) within-temperature differences between VA and RI corrected respiration were detected, with RI greater than VA in all cases. Each data point is an average of n = 8 distinct individuals and error bars are 95% confidence intervals.

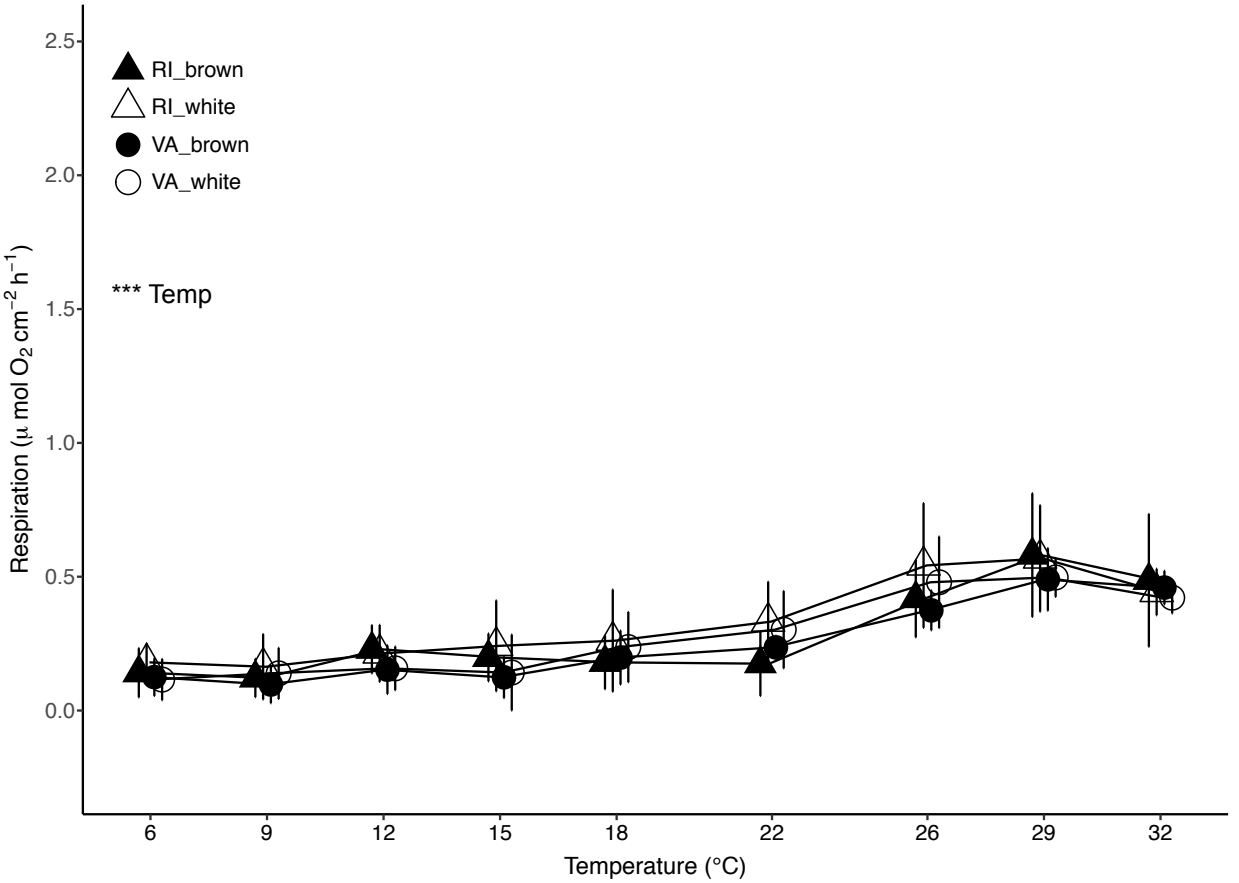

Fig. S4. ***Astrangia poculata*** **skeleton-associated commensal dark respiration.** Dark respiration rates of commensal organisms associated with the coral skeleton in brown (dark symbols) and white (open symbols) RI (triangles) and VA (circles) *A. poculata* between 6 and 32°C. Temperature had a significant effect on skeleton dark respiration rates (*** = $p < 0.0001$). Each data point is an average of n = 8 distinct individuals and error bars are 95% confidence intervals.

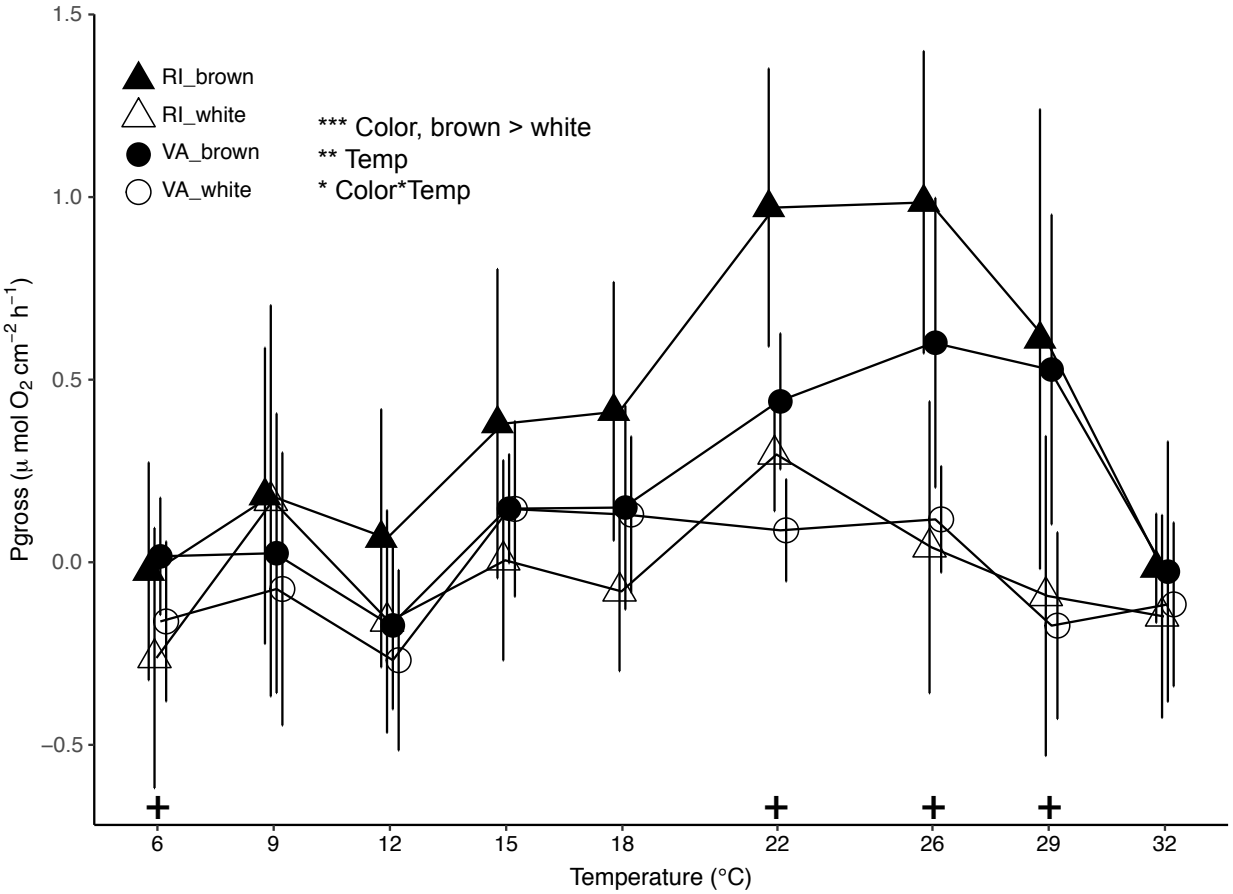

Fig. S5. ***Astrangia poculata*** **corrected gross photosynthesis.** Gross photosynthesis (net photosynthesis – dark respiration) rates of brown (dark symbols) and white (open symbols) RI (triangles) and VA (circles) *A. poculata* corrected for rates of commensals between 6 and 32°C. Color, temperature, and color*temperature all had a significant effect on gross photosynthesis rates (* = $p < 0.05$, ** = $p < 0.01$, *** = $p < 0.0001$). Plus signs above the x-axis indicate temperatures at which significant ($p < 0.05$) within-temperature differences between brown and white gross photosynthesis were detected, with brown greater than white in all cases. Each data point is an average of n = 8 distinct individuals and error bars are 95% confidence intervals.

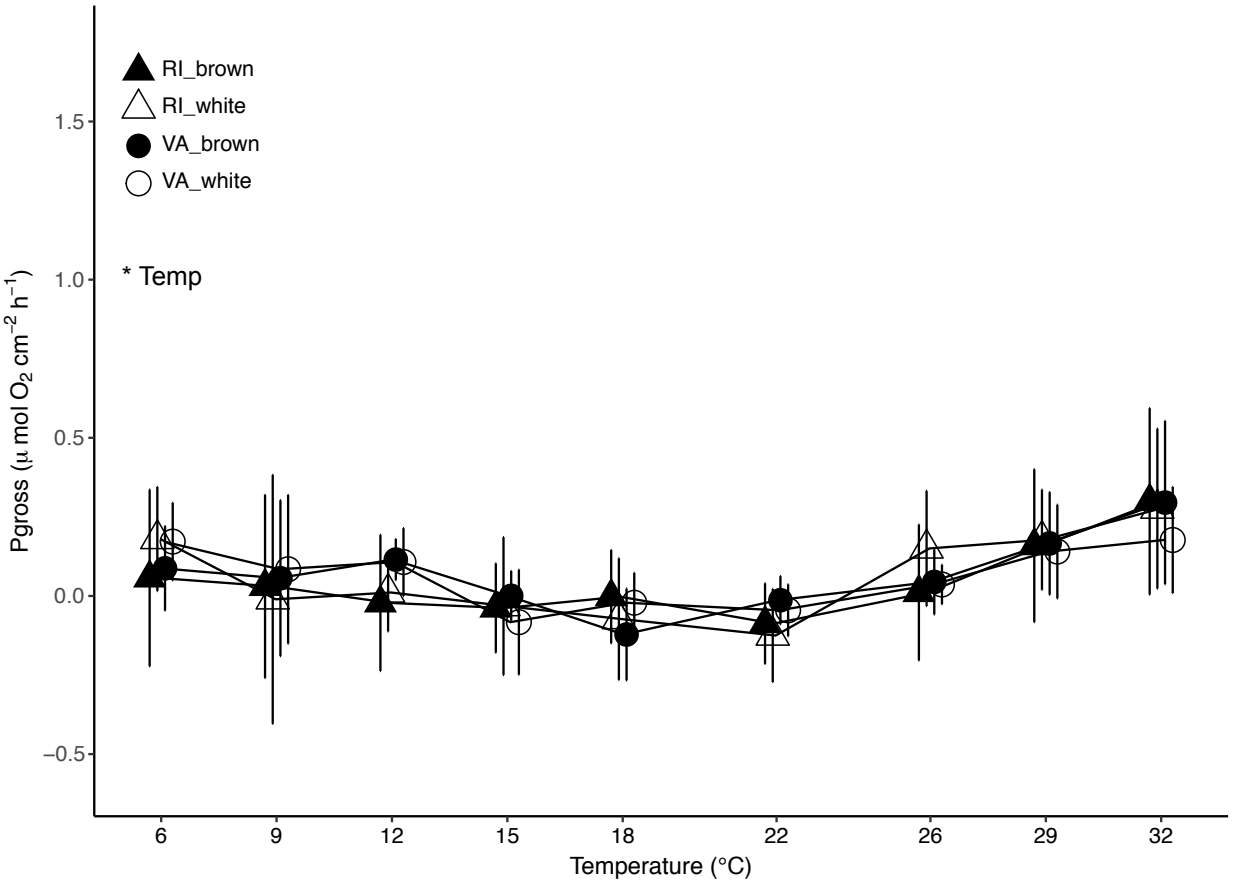

Fig. S6. ***Astrangia poculata*** **skeleton-associated commensal gross photosynthesis.** Gross photosynthesis (net photosynthesis – dark respiration) rates of commensal organisms associated with the coral skeleton in brown (dark symbols) and white (open symbols) RI (triangles) and VA (circles) *A. poculata* between 6 and 32°C. Temperature had a significant effect on commensal gross photosynthesis rates (* = $p < 0.05$). Each data point is an average of n = 8 distinct individuals and error bars are 95% confidence intervals.

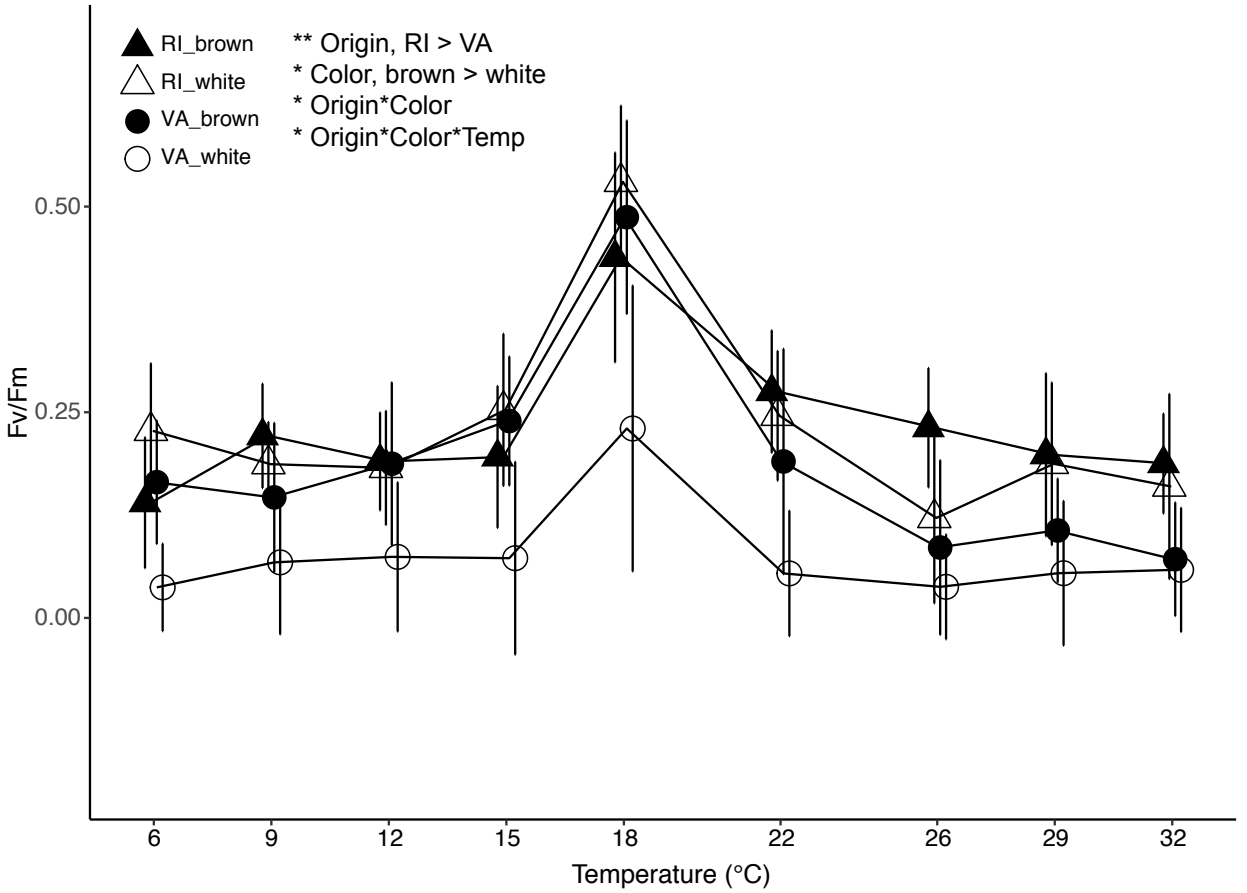

Fig. S7. ***Astrangia poculata*** **skeleton-associated commensal photochemical efficiency.** Photochemical efficiency of photosynthetic commensal organisms associated with the coral skeleton in brown (dark symbols) and white (open symbols) RI (triangles) and VA (circles) *A. poculata* between 6 and 32°C. Origin, color, origin*color and origin*color*temperature all had a significant effect on photochemical efficiency (* = $p < 0.05$, ** = $p < 0.001$). Each data point is an average of n = 8 distinct individuals, and each individual was measured in triplicate at all temperatures. Error bars are 95% confidence intervals.

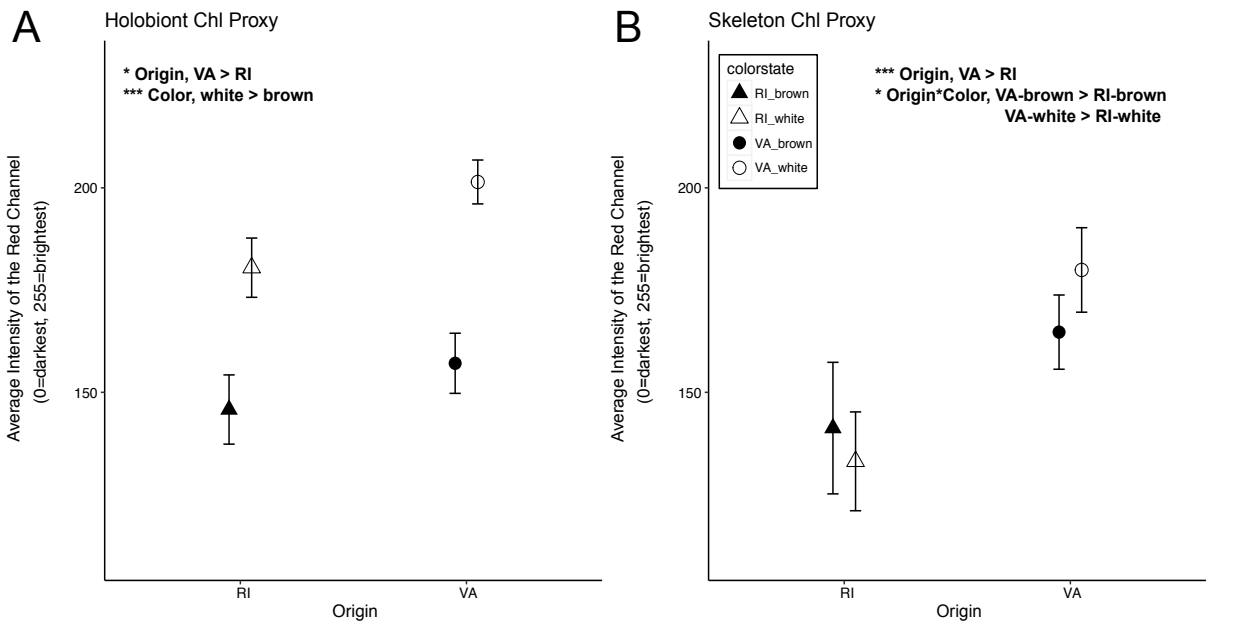

Fig. S8. ***Astrangia poculata*** **predicted chlorophyll density.** Chlorophyll density estimated from photos of *A. poculata* holobiont (A) and skeleton (B) fragments taken before the start of the heat and cold ramp experiments. Smaller intensity of the red channel = greater estimated chlorophyll density. (A) Chlorophyll density in the *A. poculata* holobiont was significantly affected by origin and color (* = $p < 0.05$; *** = $p < 0.0001$). Overall, RI holobiont fragments had more predicted chlorophyll than VA fragments and brown holobiont fragments had more predicted chlorophyll than white fragments. Each data point is an average of 16 distinct fragments, and error bars are 95% confidence intervals. (B) Chlorophyll density in the *A. poculata* skeleton was significantly different based on origin and color (* = $p < 0.05$; *** = $p < 0.0001$). Both overall and within symbiotic state, RI skeleton fragments had more predicted chlorophyll than VA fragments. Each data point is an average of 16 distinct fragments, and error bars are 95% confidence intervals.

APPENDIX B

SUPPLEMENTARY TABLES

Table S1. *Astrangia poculata* holobiont dark respiration ANOVA summary and pairwise comparisons

Holobiont Dark Respiration

Bartlett Test

Temp	K-sq	df	p-value
6	1.46	3	0.69
9	3.61	3	0.31
12	6.87	3	0.08
15	4.02	3	0.26
18	8.69	3	**0.034**
22	4.54	3	0.21
26	4.94	3	0.18
29	5.67	3	0.13
32	4.08	3	0.25

ANOVA

Model: R ~ Origin*Color*Temp + Error(Genotype/Temp)

Between-Subjects

Factor	Df	Sum_Sq	Mean_Sq	F_value	Pr(>F)
Origin	1	2.08	2.082	7.88	**0.0090**
Color	1	2.82	2.822	10.68	**0.0029**
Origin*Color	1	0.36	0.361	1.37	0.25
Residuals	28	7.40	0.264		

Within-Subjects

Factor	Df	Sum_Sq	Mean_Sq	F_value	Pr(>F)
Temp	1	62.04	62.04	338.972	**<0.0001**
Origin*Temp	1	0.15	0.15	0.805	0.38
Color*Temp	1	0.25	0.25	1.375	0.25
Origin*Color*Temp	1	0.01	0.01	0.048	0.83
Residuals	28	11.61	0.052		

Tukey's Test lsmeans Origin

Averaged over Color, Temp

Contrast	estimate	SE	df	t.ratio	p-value
RI - VA	0.3125	0.0974	142.37	3.209	**0.0016**

Tukey's Test lsmeans Color

Averaged over Origin, Temp

Contrast	estimate	SE	df	t.ratio	p-value
brown - white	-0.4074	0.0974	142.37	-4.178	**<0.0001**

Tukey's Test lsmeans Temp, only significant contrasts included

Averaged over Origin, Color

Contrast	estimate	SE	df	t.ratio	p-value
6 - 15	-0.220	0.0572	224	-3.85	**0.0047**
6 - 18	-0.478	0.0572	224	-8.36	**<0.0001**
6 - 22	-0.975	0.0572	224	-17.04	**<0.0001**
6 - 26	-1.292	0.0572	224	-22.60	**<0.0001**
6 - 29	-1.349	0.0572	224	-23.59	**<0.0001**
6 - 32	-0.955	0.0572	224	-16.70	**<0.0001**
9 - 18	-0.355	0.0572	224	-6.21	**<0.0001**
9 - 22	-0.852	0.0572	224	-14.90	**<0.0001**
9 - 26	-1.170	0.0572	224	-20.45	**<0.0001**
9 - 29	-1.227	0.0572	224	-21.45	**<0.0001**
9 - 32	-0.832	0.0572	224	-14.56	**<0.0001**
12 - 18	-0.378	0.0572	224	-6.61	**<0.0001**
12 - 22	-0.875	0.0572	224	-15.30	**<0.0001**
12 - 26	-1.193	0.0572	224	-20.85	**<0.0001**
12 - 29	-1.249	0.0572	224	-21.85	**<0.0001**
12 - 32	-0.855	0.0572	224	-14.95	**<0.0001**
15 - 18	-0.257	0.0572	224	-4.50	**0.0004**
15 - 22	-0.754	0.0572	224	-13.19	**<0.0001**
15 - 26	-1.072	0.0572	224	-18.74	**<0.0001**
15 - 29	-1.129	0.0572	224	-19.74	**<0.0001**
15 - 32	-0.735	0.0572	224	-12.85	**<0.0001**
18 - 22	-0.497	0.0572	224	-8.69	**<0.0001**
18 - 26	-0.815	0.0572	224	-14.24	**<0.0001**
18 - 29	-0.871	0.0572	224	-15.24	**<0.0001**
18 - 32	-0.477	0.0572	224	-8.34	**<0.0001**
22 - 26	-0.318	0.0572	224	-5.56	**<0.0001**
22 - 29	-0.375	0.0572	224	-6.55	**<0.0001**
26 - 32	0.337	0.0572	224	5.90	**<0.0001**
29 - 32	0.394	0.0572	224	6.89	**<0.0001**

Tukey's Test lsmeans Origin | Temp

Averaged over Color

Temp	Contrast	estimate	SE	df	t.ratio	p-value
6	RI - VA	0.170	0.061	28	2.81	**0.009**
9	RI - VA	0.236	0.129	225.42	1.82	0.0695
12	RI - VA	0.233	0.129	225.42	1.80	0.0732
15	RI - VA	0.289	0.129	225.42	2.24	**0.0263**
18	RI - VA	0.326	0.129	225.42	2.52	**0.0126**
22	RI - VA	0.574	0.129	225.42	4.44	**<0.0001**
26	RI - VA	0.514	0.129	225.42	3.97	**0.0001**
29	RI - VA	0.294	0.129	225.42	2.28	**0.0239**
32	RI - VA	0.176	0.129	225.42	1.36	0.1756

Tukey's Test lsmeans Color | Temp

Averaged over Origin

Temp	Contrast	estimate	SE	df	t.ratio	p-value
6	brown - white	-0.198	0.061	28	-3.27	**0.0029**
9	brown - white	-0.308	0.129	225.42	-2.38	**0.0182**
12	brown - white	-0.354	0.129	225.42	-2.73	**0.0068**
15	brown - white	-0.445	0.129	225.42	-3.44	**0.0007**
18	brown - white	-0.466	0.129	225.42	-3.60	**0.0004**
22	brown - white	-0.558	0.129	225.42	-4.31	**<0.0001**
26	brown - white	-0.656	0.129	225.42	-5.07	**<0.0001**
29	brown - white	-0.339	0.129	225.42	-2.62	**0.0095**
32	brown - white	-0.344	0.129	225.42	-2.66	**0.0084**

Table S2. *Astrangia poculata* skeleton dark respiration ANOVA summary and pairwise comparisons

Skeleton Dark Respiration

Bartlett Test

Temp	K-sq	df	p-value
6	0.786	3	0.853
9	2.879	3	0.411
12	0.497	3	0.920
15	5.238	3	0.155
18	3.938	3	0.268
22	8.844	3	**0.031**
26	7.486	3	0.058
29	9.231	3	**0.026**
32	20.206	3	**0.00015**

ANOVA

Model: R ~ Origin*Color*Temp + Error(Genotype/Temp)

Between-Subjects

Factor	Df	Sum_Sq	Mean_Sq	F_value	Pr(>F)
Origin	1	0.118	0.118	2.219	0.1475
Color	1	0.094	0.094	1.77	0.1941
Temp	1	0.250	0.250	4.71	**0.0386**
Origin*Color	1	0.007	0.00719	0.136	0.7154
Color*Temp	1	0.0004	0.0038	0.007	0.9328
Residuals	28	1.484	0.053		

Within-Subjects

Factor	Df	Sum_Sq	Mean_Sq	F_value	Pr(>F)
Temp	1	4.963	4.963	158.212	**<0.0001**
Origin*Temp	1	0.00	0.00	0.001	0.974
Color*Temp	1	0.00	0.00	0.008	0.929
Origin*Color*Temp	1	0.001	0.001	0.031	0.863
Residuals	30	0.941	0.031		

Tukey's Test lsmeans Temp, only significant contrasts included

Averaged over Origin, Color

Contrast	estimate	SE	df	t.ratio	p-value
6 - 22	-0.121	0.0354	222	-3.41	**0.0215**
6 - 26	-0.313	0.0354	222	-8.84	**<0.0001**
6 - 29	-0.394	0.0354	222	-11.12	**<0.0001**
6 - 32	-0.312	0.0354	222	-8.82	**<0.0001**
9 - 22	-0.131	0.0354	222	-3.70	**0.0083**
9 - 26	-0.323	0.0354	222	-9.13	**<0.0001**
9 - 29	-0.404	0.0354	222	-11.41	**<0.0001**
9 - 32	-0.322	0.0354	222	-9.10	**<0.0001**
12 - 26	-0.265	0.0354	222	-7.49	**<0.0001**
12 - 29	-0.346	0.0354	222	-9.77	**<0.0001**
12 - 32	-0.264	0.0354	222	-7.47	**<0.0001**
15 - 26	-0.277	0.0354	222	-7.82	**<0.0001**
15 - 29	-0.357	0.0354	222	-10.10	**<0.0001**
15 - 32	-0.276	0.0354	222	-7.80	**<0.0001**
18 - 26	-0.235	0.0354	222	-6.66	**<0.0001**
18 - 29	-0.315	0.0354	222	-8.95	**<0.0001**
18 - 32	-0.234	0.0354	222	-6.64	**<0.0001**
22 - 26	-0.192	0.0354	222	-5.47	**<0.0001**
22 - 29	-0.273	0.0354	222	-7.77	**<0.0001**
22 - 32	-0.191	0.0354	222	-5.45	**<0.0001**

Table S3. *Astrangia poculata* corrected dark respiration ANOVA summary and pairwise comparisons

Corrected Dark Respiration (Rcorr)

Bartlett Test

Temp	K-sq	df	p-value
6	6.99	3	0.072
9	5.16	3	0.161
12	1.13	3	0.770
15	8.57	3	**0.036**
18	9.80	3	**0.020**
22	4.37	3	0.225
26	4.76	3	0.190
29	2.90	3	0.408
32	2.30	3	0.513

ANOVA

Model: R ~ Origin*Color*Temp + Error(Genotype/Temp)

Between-Subjects

Factor	Df	Sum_Sq	Mean_Sq	F_value	Pr(>F)
Origin	1	1.564	1.56	6.361	**0.0176**
Color	1	1.504	1.50	6.117	**0.0197**
Origin*Color	1	0.024	0.02	0.099	0.7549
Residuals	28	6.884	0.25		

Within-Subjects

Factor	Df	Sum_Sq	Mean_Sq	F_value	Pr(>F)
Temp	1	22.83	22.832	169.231	**<0.0001**
Origin*Temp	1	0.08	0.08	0.594	0.447
Color*Temp	1	0.349	0.349	2.587	0.119
Origin*Color*Temp	1	0.008	0.008	0.058	0.812
Residuals	28	3.78	0.135		

Tukey's Test lsmeans Origin

Averaged over Color, Temp

Contrast	estimate	SE	df	t.ratio	p-value
RI - VA	0.281	0.0918	134.51	3.065	**0.0026**

Tukey's Test lsmeans Color

Averaged over Origin, Temp

Contrast	estimate	SE	df	t.ratio	p-value
brown - white	-0.315	0.0918	134.51	-3.426	**0.0008**

Tukey's Test lsmeans Temp, only significant contrasts included)

Averaged over Origin, Color

Contrast	estimate	SE	df	t.ratio	p-value
6 - 18	-0.293	0.0531	224	-5.51	**<0.0001**
6 - 22	-0.725	0.0531	224	-13.64	**<0.0001**
6 - 26	-0.846	0.0531	224	-15.92	**<0.0001**
6 - 29	-0.822	0.0531	224	-15.47	**<0.0001**
6 - 32	-0.509	0.0531	224	-9.59	**<0.0001**
9 - 18	-0.196	0.0531	224	-3.69	**0.0085**
9 - 22	-0.628	0.0531	224	-11.83	**<0.0001**
9 - 26	-0.750	0.0531	224	-14.11	**<0.0001**
9 - 29	-0.726	0.0531	224	-13.66	**<0.0001**
9 - 32	-0.413	0.0531	224	-7.77	**<0.0001**
12 - 18	-0.271	0.0531	224	-5.09	**<0.0001**
12 - 22	-0.703	0.0531	224	-13.23	**<0.0001**
12 - 26	-0.824	0.0531	224	-15.51	**<0.0001**
12 - 29	-0.800	0.0531	224	-15.06	**<0.0001**
12 - 32	-0.488	0.0531	224	-9.18	**<0.0001**
15 - 18	-0.149	0.0531	224	-2.81	**0.0422**
15 - 22	-0.582	0.0531	224	-10.94	**<0.0001**
15 - 26	-0.703	0.0531	224	-13.22	**<0.0001**
15 - 29	-0.679	0.0531	224	-12.78	**<0.0001**
15 - 32	-0.366	0.0531	224	-6.89	**<0.0001**
18 - 22	-0.432	0.0531	224	-8.14	**<0.0001**
18 - 26	-0.553	0.0531	224	-10.42	**<0.0001**
18 - 29	-0.530	0.0531	224	-9.97	**<0.0001**
18 - 32	-0.217	0.0531	224	-4.08	**0.002**
22 - 32	0.215	0.0531	224	4.05	**0.0025**
26 - 32	0.336	0.0531	224	6.33	**<0.0001**
29 - 32	0.313	0.0531	224	5.88	**<0.0001**

Tukey's Test lsmeans Origin | Temp

Averaged over Color

Temp	Contrast	estimate	SE	df	t.ratio	p-value
6	RI - VA	0.147	0.058	28	2.52	**0.018**
9	RI - VA	0.227	0.121	219.45	1.87	0.063
12	RI - VA	0.186	0.121	219.45	1.53	0.13
15	RI - VA	0.258	0.121	219.45	2.13	**0.034**
18	RI - VA	0.324	0.121	219.45	2.67	**0.0081**
22	RI - VA	0.590	0.121	219.45	4.87	**<0.0001**
26	RI - VA	0.452	0.121	219.45	3.73	**0.0002**
29	RI - VA	0.205	0.121	219.45	1.69	0.092
32	RI - VA	0.143	0.121	219.45	1.18	0.24

Table S4. *Astrangia poculata* holobiont gross photosynthesis ANOVA summary and pairwise comparisons

Holobiont Gross Photosynthesis (Pgross)

Bartlett Test

Temp	K-sq	df	p-value
6	3.87	3	0.28
9	1.79	3	0.62
12	1.29	3	0.73
15	11.57	3	**0.01**
18	1.68	3	0.64
22	5.84	3	0.12
26	3.66	3	0.30
29	5.32	3	0.15
32	5.56	3	0.14

ANOVA

Model: Pgross ~ Origin*Color*Temp + Error(Genotype/Temp)

Between-Subjects

Factor	Df	Sum_Sq	Mean_Sq	F_value	Pr(>F)
Origin	1	0.609	0.609	3.459	0.0734
Color	1	7.567	7.567	42.957	**<0.0001**
Origin*Color	1	0.255	0.255	1.447	0.239
Residuals	28	4.932	0.176		

Within-Subjects

Factor	Df	Sum_Sq	Mean_Sq	F_value	Pr(>F)
Temp	1	4.636	4.636	21.6	**<0.0001**
Origin*Temp	1	0.105	0.105	0.489	0.490
Color*Temp	1	1.754	1.754	8.17	**0.00796**
Origin*Color*Temp	1	0	0	0.001	0.975
Residuals	28	6.001	0.215		

Tukey's Test lsmeans Color

Averaged over Origin, Temp

Contrast	estimate	SE	df	t.ratio	p-value
brown - white	0.544	0.109	231.63	4.98	**<0.0001**

Tukey's Test lsmeans Temp, only significant contrasts included

Averaged over Origin, Color

Contrast	estimate	SE	df	t.ratio	p-value
6 - 22	-0.365	0.0732	224	-4.98	**0.0001**
6 - 26	-0.481	0.0732	224	-6.57	**<0.0001**
6 - 29	-0.363	0.0732	224	-4.96	**0.0001**
9 - 22	-0.265	0.0732	224	-3.62	**0.0106**
9 - 26	-0.381	0.0732	224	-5.21	**<0.0001**
9 - 29	-0.264	0.0732	224	-3.60	**0.0115**
12 - 22	-0.462	0.0732	224	-6.32	**<0.0001**
12 - 26	-0.578	0.0732	224	-7.90	**<0.0001**
12 - 29	-0.461	0.0732	224	-6.29	**<0.0001**
12 - 32	-0.267	0.0732	224	-3.65	**0.0098**
15 - 22	-0.250	0.0732	224	-3.41	**0.0216**
15 - 26	-0.365	0.0732	224	-4.99	**<0.0001**
15 - 29	-0.248	0.0732	224	-3.39	**0.0233**
18 - 22	-0.284	0.0732	224	-3.87	**0.0044**
18 - 26	-0.399	0.0732	224	-5.46	**<0.0001**
18 - 29	-0.282	0.0732	224	-3.85	**0.0048**
26 - 32	0.311	0.0732	224	4.25	**0.001**

Tukey's Test lsmeans Color | Temp

Averaged over Origin

Temp	Contrast	estimate	SE	df	t.ratio	p-value
6	brown - white	0.324	0.049	28	6.55	**<0.0001**
9	brown - white	0.282	0.155	251.81	1.83	0.069
12	brown - white	0.369	0.155	251.81	2.39	**0.018**
15	brown - white	0.446	0.155	251.81	2.89	**0.0042**
18	brown - white	0.512	0.155	251.81	3.31	**0.0011**
22	brown - white	0.770	0.155	251.81	4.98	**<0.0001**
26	brown - white	0.869	0.155	251.81	5.62	**<0.0001**
29	brown - white	0.926	0.155	251.81	5.99	**<0.0001**
32	brown - white	0.402	0.155	251.81	2.60	**0.0099**

Table S5. *Astrangia poculata* skeleton gross photosynthesis ANOVA summary and pairwise comparisons

Skeleton Gross Photosynthesis (Pgross)

Bartlett Test

Temp	K-sq	df	p-value
6	6.04	3	0.11
9	2.31	3	0.51
12	9.30	3	**0.026**
15	6.17	3	0.10
18	3.12	3	0.37
22	4.04	3	0.26
26	10.38	3	**0.016**
29	2.18	3	0.54
32	2.05	3	0.56

ANOVA

Model: Pgross ~ Origin*Color*Temp + Error(Genotype/Temp)

Between-Subjects

Factor	Df	Sum_Sq	Mean_Sq	F_value	Pr(>F)
Origin	1	0.012	0.0124	0.273	0.61
Color	1	0.002	0.0017	0.037	0.85
Temp	2	0.024	0.0236	0.522	0.48
Origin*Color	1	0.010	0.0098	0.217	0.65
Color*Temp	1	0.002	0.0015	0.034	0.86
Residuals	28	1.268	0.0453		

Within-Subjects

Factor	Df	Sum_Sq	Mean_Sq	F_value	Pr(>F)
Temp	1	0.464	0.464	6.795	**0.014**
Origin*Temp	1	0.071	0.071	1.035	0.32
Color*Temp	1	0.046	0.046	0.673	0.42
Origin*Color*Temp	1	0.014	0.014	0.209	0.65
Residuals	30	11.706	0.053		

Tukey's Test lsmeans Temp, only significant contrasts included

Averaged over Origin, Color

Contrast	estimate	SE	df	t.ratio	p-value
6 - 18	0.179	0.0570	222	3.14	**0.050**
6 - 22	0.190	0.0579	222	3.31	**0.030**
9 - 32	-0.223	0.0579	222	-3.89	**0.0041**
12 - 32	-0.211	0.0579	222	-3.67	**0.0092**
15 - 29	-0.201	0.0579	222	-3.49	**0.017**
15 - 32	-0.302	0.0579	222	-5.25	**<0.0001**
18 - 29	-0.217	0.0575	222	-3.78	**0.0062**
18 - 32	-0.318	0.0575	222	-5.54	**<0.0001**
22 - 29	-0.229	0.0570	222	-4.01	**0.0027**
22 - 32	-0.330	0.0570	222	-5.78	**<0.0001**
26 - 32	-0.201	0.0570	222	-3.53	**0.015**

Table S6. *Astrangia poculata* corrected gross photosynthesis ANOVA summary and pairwise comparisons

Corrected Gross Photosynthesis (Pgross)

Bartlett Test

Temp	K-sq	df	p-value
6	4.48	3	0.21
9	1.19	3	0.76
12	1.55	3	0.67
15	6.84	3	0.077
18	2.33	3	0.51
22	9.31	3	**0.025**
26	6.98	3	0.07
29	4.93	3	0.18
32	4.85	3	0.18

ANOVA

Model: Pgross ~ Origin*Color*Temp + Error(Genotype/Temp)

Between-Subjects

Factor	Df	Sum_Sq	Mean_Sq	F_value	Pr(>F)
Origin	1	0.83	0.83	3.03	0.093
Color	1	7.53	7.53	27.421	**<0.0001**
Origin*Color	1	0.71	0.71	2.574	0.12
Residuals	28	7.69	0.28		

Within-Subjects

Factor	Df	Sum_Sq	Mean_Sq	F_value	Pr(>F)
Temp	1	2.12	2.12	10.91	**0.0026**
Origin*Temp	1	0.00	0.00	0.021	0.89
Color*Temp	1	1.27	1.27	6.561	**0.016**
Origin*Color*Temp	1	0.02	0.02	0.086	0.77
Residuals	28	5.43	0.19		

Tukey's Test lsmeans Color

Averaged over Origin, Temp

Contrast	estimate	SE	df	t.ratio	p-value
brown - white	0.439	0.138	233.21	3.181	**0.0017**

Tukey's Test lsmeans Temp, only significant contrasts included

Averaged over Origin, Color

Contrast	estimate	SE	df	t.ratio	p-value
6 - 22	-0.557	0.0925	224	-6.02	**<0.0001**
6 - 26	-0.545	0.0925	224	-5.88	**<0.0001**
6 - 29	-0.326	0.0925	224	-3.53	**0.015**
9 - 22	-0.373	0.0925	224	-4.03	**0.0024**
9 - 26	-0.361	0.0925	224	-3.90	**0.004**
12 - 15	-0.304	0.0925	224	-3.28	**0.032**
12 - 22	-0.583	0.0925	224	-6.30	**<0.0001**
12 - 26	-0.571	0.0925	224	-6.17	**<0.0001**
12 - 29	-0.353	0.0925	224	-3.81	**0.0055**
18 - 22	-0.295	0.0925	224	-3.19	**0.042**
22 - 32	0.525	0.0925	224	5.67	**<0.0001**
26 - 32	0.513	0.0925	224	5.54	**<0.0001**
29 - 32	0.295	0.0925	224	3.18	**0.04**

Tukey's Test lsmeans Color | Temp

Averaged over Origin

Temp	Contrast	estimate	SE	df	t.ratio	p-value
6	brown - white	0.323	0.062	28	5.24	**<0.0001**
9	brown - white	0.171	0.195	251.7	0.88	0.38
12	brown - white	0.277	0.195	251.7	1.42	0.16
15	brown - white	0.303	0.195	251.7	1.55	0.12
18	brown - white	0.372	0.195	251.7	1.91	0.058
22	brown - white	0.630	0.195	251.7	3.23	**0.0014**
26	brown - white	0.830	0.195	251.7	4.25	**<0.0001**
29	brown - white	0.818	0.195	251.7	4.19	**<0.0001**
32	brown - white	0.226	0.195	251.7	1.16	0.25

Table S7. *Astrangia poculata* holobiont photochemical efficiency (F_v/F_m) ANOVA summary and pairwise comparisons

Holobiont Photochemical Efficiency (Fv/Fm)

Bartlett Test Model: FvFm ~ colorstate

Temp	K-sq	df	p-value
6	1.06	3.00	0.79
9	5.99	3.00	0.11
12	1.94	3.00	0.58
15	6.80	3.00	0.08
18	6.31	3.00	0.10
22	3.55	3.00	0.31
26	0.62	3.00	0.89
29	5.13	3.00	0.16
32	1.35	3.00	0.72

ANOVA

Model: FvFm ~ Origin*Color*Temp + Error (Genotype/Temp)

Between-Subjects

Factor	Df	Sum_Sq	Mean_Sq	F_value	Pr(>F)
Origin	1	0.0001	0.0001	0.006	0.94
Color	1	1.972	1.972	9.57	**1.13e-10**
Origin:Color	1	0.007	0.0066	0.33	0.57
Residuals	28	0.560	0.02		

Within-Subjects

Factor	Df	Sum_Sq	Mean_Sq	F_value	Pr(>F)
Temp	1	0.156	0.156	13.06	**0.0012**
Origin:Temp	1	0.015	0.151	1.265	0.27
Color:Temp	1	0.153	0.153	12.802	**0.0013**
Origin:Color:Temp	1	0.004	0.004	0.315	0.58
Residuals	28	0.338	0.012		

Tukey's Telsmeans of Color

Averaged over Origin,Temp

Contrast	estimate	SE	df	t.ratio	p-value
brown - white	0.146	0.0324	188.52	4.762	**<.0001**

Tukey's Telsmeans of Color | Temp

Averaged over Origin,Temp

	Contrast	estimate	SE	df	t.ratio	p-value
6	brown - white	0.165	0.0167	28	9.93	**<.0001**
9	brown - white	0.197	0.0422	246.9	4.66	**<.0001**
12	brown - white	0.225	0.0422	246.9	5.33	**<.0001**
15	brown - white	0.232	0.0422	246.9	5.50	**<.0001**
18	brown - white	0.119	0.0422	246.9	2.83	**0.0051**
22	brown - white	0.108	0.0422	246.9	2.57	**0.0108**
26	brown - white	0.107	0.0422	246.9	2.53	**0.0121**
29	brown - white	0.106	0.0422	246.9	2.51	**0.0128**
32	brown - white	0.059	0.0422	246.9	1.39	0.1644

Tukey's Telsmeans of Temp, only significant contrasts included

Averaged over Origin, Color

Contrast	estimate	SE	df	t.ratio	p-value
6 - 12	-0.062	0.0194	224	-3.21	0.040
6 - 15	-0.139	0.0194	224	-7.16	**<.0001**
6 - 18	-0.292	0.0194	224	-15.09	**<.0001**
6 - 22	-0.132	0.0194	224	-6.84	**<.0001**
6 - 26	-0.119	0.0194	224	-6.13	**<.0001**
6 - 29	-0.106	0.0194	224	-5.47	**<.0001**
6 - 32	-0.077	0.0194	224	-3.99	**0.003**
9 - 15	-0.095	0.0194	224	-4.93	**0.0001**
9 - 18	-0.250	0.0194	224	-12.86	**<0.0001**
9 - 22	-0.089	0.0194	224	-4.61	**0.0002**
9 - 26	-0.075	0.0194	224	-3.90	**0.004**
9 - 29	-0.063	0.0194	224	-3.24	**0.04**
12 - 15	-0.076	0.0194	224	-3.95	**0.003**
12 - 18	-0.230	0.0194	224	-11.88	**<0.0001**
12 - 22	-0.070	0.0194	224	-3.62	**0.01**
15 - 18	-0.154	0.0194	224	-7.93	**<0.0001**
15 - 32	0.061	0.0194	224	3.17	**0.05**
18 - 22	0.160	0.0194	224	8.26	**<0.0001**
18 - 26	0.174	0.0194	224	8.97	**<0.0001**
18 - 29	0.186	0.0194	224	9.62	**<0.0001**
18 - 32	0.215	0.0194	224	11.10	**<0.0001**

Table S8. *Astrangia poculata* skeleton photochemical efficiency (F_v/F_m) ANOVA summary and pairwise comparisons

Skeleton Photochemical Efficiency (Fv/Fm)

Bartlett Test Model: FvFm ~ colorstate

Temp	K-sq	df	p-value
6	1.40	3	0.71
9	2.74	3	0.43
12	2.11	3	0.55
15	1.23	3	0.75
18	4.26	3	0.24
22	3.93	3	0.27
26	2.48	3	0.48
29	1.58	3	0.66
32	3.08	3	0.38

ANOVA

Model: FvFm ~ Origin*Color*Temp + Error (Genotype/Temp)

Between-Subjects

Factor	Df	Sum_Sq	Mean_Sq	F_value	Pr(>F)
Origin	1	0.73	0.73	16.49	**0.0004**
Color	1	0.21	0.21	4.81	**0.037**
Temp	1	0.02	0.02	0.56	0.46
Origin:Color	1	0.23	0.23	5.14	**0.03**
Color:Temp	1	0.04	0.04	0.96	0.34
Residuals	28	1.20	0.04		

Within-Subjects

Factor	Df	Sum_Sq	Mean_Sq	F_value	Pr(>F)
Temp	1	0.0369	0.0369	2.36	0.14
Origin:Temp	1	0.0235	0.0235	1.499	0.23
Color:Temp	1	0.0015	0.0015	0.095	0.76
Origin:Color:Temp	1	0.1058	0.1058	6.759	**0.014**
Residuals	30	0.4694	0.0157		

Tukey's Test lsmeans of Origin

Averaged over Color, Temp

Contrast	estimate	SE	df	t.ratio	p-value
RI - VA	0.12065	0.03856	131.09	3.129	**0.0022**

Tukey's Test lsmeans of Color

Averaged over Origin, Temp

Contrast	estimate	SE	df	t.ratio	p-value
brown - white	0.05587	0.12598	30.28	0.443	0.66

Tukey's Test lsmeans of Origin | Color

Averaged over Origin, Color

Color	Contrast	estimate	SE	df	t.ratio	p-value
brown	RI - VA	0.124	0.0545	130.94	2.269	**0.025**
white	RI - VA	0.118	0.0546	131.25	2.156	**0.033**

Tukey's Test lsmeans of Origin | Temp | Color, only significant contrasts included

Averaged over Origin, Color

Temp	Contrast	estimate	SE	df	t.ratio	p-value
6	RI white - VA white	0.04	0.03	27.00	4.52	**0.0006**
18	RI white - VA white	0.25	0.07	215.30	3.53	**0.0028**
26	RI brown - VA brown	0.24	0.07	215.66	3.29	**0.0065**
32	RI brown - VA brown	0.21	0.07	215.66	2.88	**0.0226**

Table S9. *Astrangia poculata* thermal optima (T_{opt}) ANOVA summary and pairwise comparisons

Thermal Optimum (Topt, calculated using corrected dark respiration rates)

Bartlett Test Model: Topt ~ colorstate

K-sq	df	p-value
6.42	3	0.093

ANOVA

Model: Topt ~ Origin*Color

Factor	df	Sum_Sq	Mean_Sq	F_value	Pr(>F)
origin	1	186.2	186.22	7.19	**0.013**
color	1	0	0.04	0.00	0.97
origin:color	1	16.3	16.31	0.63	0.44
Residuals	23	596.1	25.92		

Tukey's Test lsmeans of origin

Averaged over Color

Contrast	estimate	SE	df	t.ratio	p-value
RI - VA	-5.32	1.96	23	-2.71	**0.013**

Table S10. *Astrangia poculata* holobiont (A) and skeleton (B) color ANOVA summary and pairwise comparisons

A. Holobiont Coral Color

Bartlett Test: Model: AvgRedChannel ~ colorstate

K-sq	df	p-value
13.77	3	0.0032

ANOVA

Model: AvgRedChannel ~ Origin*Color

Factor	Df	Sum_Sq	Mean_Sq	F_value	Pr(>F)
origin	1	2950	2950	9.60	**0.00296**
color	1	25824	25824	84.0	**<0.0001**
origin:color	1	420	420	1.37	0.24706
Residuals	60	18432	307		

Tukey's Test: lsmeans of color

Averaged over Origin

Contrast	estimate	SE	df	t.ratio	p-value
brown - white	-40.18	4.38	60	-9.17	**<.0001**

Tukey's Test: lsmeans of origin

Averaged over Color

Contrast	estimate	SE	df	t.ratio	p-value
ri - va	-13.58	4.38	60	-3.10	**0.003**

B. Skeleton Coral Color

Bartlett Test: Model: AvgRedChannel ~ colorstate

K-sq	df	p-value
5.55	3	0.14

ANOVA

Model: AvgRedChannel ~ Origin*Color

Factor	Df	Sum_Sq	Mean_Sq	F_value	Pr(>F)
origin	1	19753	19753	37.78	**<0.0001**
color	1	200	200	0.383	0.54
origin:color	1	2177	2177	4.16	**0.046**
Residuals	60	31372	523		

Tukey's Test: lsmeans of origin

Averaged over Color

Contrast	estimate	SE	df	t.ratio	p-value
ri - va	-35.1	5.72	60	-6.146	**<0.0001**

Tukey's Test: lsmeans of origin*color

Contrast	estimate	SE	df	t.ratio	p-value
ri, brown - va, brown	-23.47	8.045	60	-2.90	**0.026**
ri, brown - ri, white	8.13	8.045	60	1.01	0.75
ri, brown - va, white	-38.68	8.045	60	-4.78	**0.0001**
va, brown - ri, white	31.60	8.045	60	3.91	**0.0013**
va, brown - va, white	-15.20	8.045	60	-1.88	0.25
ri, white - va, white	-46.80	8.045	60	-5.79	**<0.0001**

VITA

Hannah Elise Aichelman
Department of Biological Sciences, Old Dominion University
110 Mills Godwin Life Sciences Building, Norfolk, Virginia, 23529

EDUCATION

OLD DOMINION UNIVERSITY, NORFOLK, VIRGINIA
Master of Science, Department Biological Sciences, August 2018
Advisor: Dr. Daniel Barshis

UNIVERSITY OF NORTH CAROLINA, CHAPEL HILL
Bachelor of Science, May 2014
Major: Environmental Science
Advisor: Dr. Karl Castillo

PUBLICATIONS

Rippe JP, Baumann JH, **Aichelman HE**, DeLeener D, Friedlander E and KD Castillo (In Review) Colony-level variation in coral growth overshadows regional patterns on the Florida Keys Reef Tract. *Global Change Biology*

Baumann JH, Ries JB, Rippe JP, Courtney TA, **Aichelman HE**, Westfield I and KD Castillo (In Review) Declining skeletal extension in near shore corals across the Belize Mesoamerican Barrier Reef System. *Scientific Reports*

Baumann JH, Davies SW, **Aichelman HE** and KD Castillo (2018) Coral *Symbiodinium* community composition across the Belize Mesoamerican Barrier Reef System is influenced by host species and thermal variability. *Microbial Ecology*. 75(4), 903-915.

Aichelman HE, Townsend J, Courtney T, Baumann J, Davies SW and KD Castillo (2016) Heterotrophy Mitigates the Response of the Temperate Coral *Oculina arbuscula* to Temperature Stress. *Ecology and Evolution.* 6(18), 6758-6769.

Baumann JH, Townsend JE, Courtney TA, **Aichelman HE**, Davies SW, Lima FP and KD Castillo (2016) Temperature Regimes Impact Coral Assemblages along Environmental Gradients on Lagoonal Reefs in Belize. *PLoS ONE.* 11(9), e0162098.

PROFESSIONAL EXPERIENCE

2016-2017	**Advanced Science Communication Seminar,** *Virginia Institute of Marine Sciences*
2014-2016	**Lab Manager,** *University of North Carolina-Chapel Hill*
2014	**Deckhand/Educator, S/V Denis Sullivan,** *Discovery World, Milwaukee, WI*
2013-2014	**Undergraduate Research Assistant**, *University of North Carolina-CH*
2013	**NSF Research Experience for Undergraduates (REU),** *Mote Marine Lab, Sarasota, FL*

GRANTS

AAUS Hollis Gear Award. $1250 (2017).
ODU Biology Graduate Student (BGSO) Research Award. $300 (2017).
PADI Foundation. $6,300 (2017).
ODU Biology Graduate Student Organization (BGSO) Research Award. $200 (2016).
Virginia Sea Grant Graduate Research Fellowship. $80,000 (2016-2018).
National Science Foundation Graduate Research Fellowship Program (NSF GRFP). $102,000 (2016-2021).